



6-1974

## The Origin and Nature of Flash Weld Defects in Iron-Nickel Base Superalloys

Ronald William Gunkel  
*University of Tennessee - Knoxville*

Follow this and additional works at: [https://trace.tennessee.edu/utk\\_gradthes](https://trace.tennessee.edu/utk_gradthes)



Part of the [Metallurgy Commons](#)

### Recommended Citation

Gunkel, Ronald William, "The Origin and Nature of Flash Weld Defects in Iron-Nickel Base Superalloys. " Master's Thesis, University of Tennessee, 1974.  
[https://trace.tennessee.edu/utk\\_gradthes/1234](https://trace.tennessee.edu/utk_gradthes/1234)

This Thesis is brought to you for free and open access by the Graduate School at TRACE: Tennessee Research and Creative Exchange. It has been accepted for inclusion in Masters Theses by an authorized administrator of TRACE: Tennessee Research and Creative Exchange. For more information, please contact [trace@utk.edu](mailto:trace@utk.edu).

To the Graduate Council:

I am submitting herewith a thesis written by Ronald William Gunkel entitled "The Origin and Nature of Flash Weld Defects in Iron-Nickel Base Superalloys." I have examined the final electronic copy of this thesis for form and content and recommend that it be accepted in partial fulfillment of the requirements for the degree of Master of Science, with a major in Materials Science and Engineering.

Carl D. Lundin, Major Professor

We have read this thesis and recommend its acceptance:

C. R. Brooks, W. T. Becker

Accepted for the Council:

Carolyn R. Hodges

Vice Provost and Dean of the Graduate School

(Original signatures are on file with official student records.)

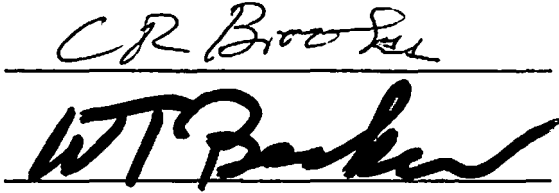
To the Graduate Council:

I am submitting herewith a thesis written by Ronald William Gunkel entitled "The Origin and Nature of Flash Weld Defects in Iron-Nickel Base Superalloys." I recommend that it be accepted in partial fulfillment of the requirements for the degree of Master of Science, with a major in Metallurgical Engineering.

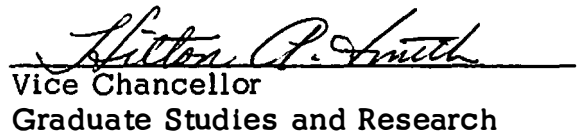


Carl D. Lundin, Major Professor

We have read this thesis  
and recommend its acceptance:



Accepted for the Council:



Hilton P. Smith  
Vice Chancellor  
Graduate Studies and Research

**THE ORIGIN AND NATURE OF FLASH WELD DEFECTS  
IN IRON-NICKEL BASE SUPERALLOYS**

**A Thesis  
Presented for the  
Master of Science  
Degree  
The University of Tennessee**

**Ronald William Gunkel**

**June 1974**

## ACKNOWLEDGEMENTS

The author wishes to express his sincere thanks to Dr. C. D. Lundin for his help and guidance during the course of this research project. The author would like to thank Mr. Bob McGill for his interest and guidance in scanning electron microscopy and Mr. Bill Leslie of Oak Ridge National Laboratory for his assistance and advise in preparing the metallographic specimens. Without the materials and assistance provided by American Welding and Manufacturing Company, the research reported in this thesis would not have been possible. The author is also indebted to the Department of Chemical and Metallurgical Engineering for its financial support during the course of this investigation. Finally, the author would like to thank his wife Joyce for her interest and support throughout his graduate program.

## ABSTRACT

The purpose of this investigation is to determine the nature and morphology of weld defects on the fracture surfaces of flash welded high temperature, high strength alloys. Emphasis is on the material-related phenomena instead of the more commonly studied welding process variables.

Samples were fractured in a slow bend test using three-point loading. The resulting fracture surfaces were examined in a scanning electron microscope, and elemental analysis of distinctive fracture features was determined using the ancillary energy dispersive x-ray system. When the fracture surface analyses were completely documented, metallographic sections through distinctive features were examined using a bench metallograph.

The base materials used in this study exhibited banded microstructures in which the particle/segregate bands were elongated primarily parallel to the longitudinal axis. The orientation between these banded microstructural features and a propagating crack influence the fracture path. This, in turn, determines the fracture surface appearance and weld ductility.

A dimpled appearance predominated on every fracture surface studied. One exception to the microvoid fracture mechanism is crack propagation through an entrapped oxide film which formed during flashing.

A flat spot is created where fracture occurs by this means. Oxides of aluminum and titanium are the primary constituents of the defect which has this morphology. All other flat spots and streaks are caused by bands of high particle density which become preferential paths for fracture propagation. The total strain to fracture is very low in these regions even though fracture occurs by initiation and coalescence of microvoids. Thus, flat spots and streaks appear flat at low magnification but most exhibit dimples at high magnification. These dimples are considerably smaller than those on the adjacent low particle density fracture surface.

In conclusion, this investigation showed that the base material microstructure can exert a marked influence on the occurrence of flash weld defects.

## TABLE OF CONTENTS

CHAPTER	PAGE
I. INTRODUCTION AND HISTORICAL REVIEW . . . . .	1
Flash Welding Process Variables . . . . .	3
Flash Weld Defects . . . . .	6
Object . . . . .	16
II. MATERIALS AND PROCEDURES . . . . .	17
Materials . . . . .	17
Equipment . . . . .	19
Experimental Technique . . . . .	25
III. RESULTS AND DISCUSSION . . . . .	27
Materials . . . . .	28
General . . . . .	28
Materials used in this study. . . . .	28
Effect of Microstructure on Fracture Propagation . . . . .	34
Macroscopic Examination of Fracture Surfaces . . . . .	45
Microscopic Examination of Weld Defects . . . . .	50
IV. CONCLUSIONS . . . . .	81
V. FUTURE WORK . . . . .	84
LIST OF REFERENCES . . . . .	86



CHAPTER	PAGE
BIBLIOGRAPHY . . . . .	91
APPENDIX . . . . .	93
VITA. . . . .	104

## LIST OF FIGURES

FIGURE	PAGE
1. Macrograph of the Mating Fracture Surfaces from a Flash Welded Hastelloy X Sample . . . . .	11
2. Scanning Electron Micrograph of Some Flat Areas on the Fracture Surface of a Flash Welded Hastelloy X Sample . . . . .	12
3. Higher Magnification Scanning Electron Micrograph of Flat Areas Seen in Figure 2 . . . . .	13
4. Schematic Diagram of Scanning Electron Microscope . . . .	22
5. Signals Generated in the Scanning Electron Microscope . .	23
6. Micrographs of Banding in Waspaloy Base Material. . . . .	29
7. Micrograph of Longitudinal Section from Hastelloy X Base Material. . . . .	31
8. High Magnification Micrographs of Bands from Figure 7 . .	32
9. Longitudinal Microstructure of Inconel 718 Which Is Also Representative of N-155 and Inconel 625 . . . . .	33
10. Schematic Diagram of Flash Weld . . . . .	38
11. Carbide Population at Various Distances from the Weld Interface . . . . .	40

FIGURE	PAGE
12. Constitutional Liquation in Flash Weld Hastelloy X	
Specimen . . . . .	41
13. Effect of Flash Welding Upset Upon the Fracture Path	
for Slow Bend Specimens Having Banded	
Microstructures. . . . .	43
14. Effect of Fracture Propagation Direction Upon Fracture	
Face Appearance . . . . .	46
15. Fracture Faces of Two Different Flash Welded Joints	
Made in Waspaloy . . . . .	48
16. Fracture Faces of Two Different Flash Welded Joints	
Made in Inconel 625 . . . . .	49
17. Fracture Faces of Two Different Flash Welded Joints	
Made in N-155 . . . . .	51
18. Fracture Faces of Two Different Flash Welded Joints	
Made in Inconel 718 . . . . .	52
19. SEM Micrographs of Streak on Waspaloy Fracture	
Surface . . . . .	54
20. SEM Micrographs Comparing Dimple Size on the Streak	
and Adjacent Area at 500X . . . . .	55
21. SEM Micrograph of Streak at 2000X . . . . .	56
22. SEM Micrograph of Streaks on the Fracture Face of an	
Inconel 718 Weld Sample . . . . .	58

FIGURE	PAGE
23. Higher Magnification SEM Micrographs of One Streak	
Shown in Figure 22 . . . . .	59
24. SEM Micrograph of a Fractured Intermediate Width	
Particle/Segregate Band . . . . .	62
25. Higher Magnification SEM Micrographs of Feature	
Shown in Figure 24 . . . . .	64
26. Microstructure at Two Locations Along the Sectioning	
Line Shown in Figure 24 . . . . .	65
27. Flat Spot Caused by Broad, Flat Microstructural	
Particle Bands. . . . .	67
28. SEM Micrographs Comparing the Dimple Size of the	
Rough and Flat Areas of Figure 27. . . . .	68
29. SEM Micrographs Showing Dark Areas on the Fracture	
Face of an Inconel 625 Weld Sample . . . . .	70
30. High Magnification SEM and Light Micrographs of the	
Dark Area Shown in Figure 29. . . . .	71
31. Flat Spot on Fracture Face of a Hastelloy X Flash Weld. . .	72
32. Flat Spot Shown in Figure 31 at Higher Magnifications . . .	74
33. Light Micrographs Showing Typical Areas Along the	
Interface of the Flat Spot Shown in Figure 31. . . . .	75
34. SEM Micrographs of Pockmarked Oxide Film on a Flat	
Spot. . . . .	76

FIGURE	PAGE
35. SEM Micrographs of "Blob" Found on an N-155 Fracture Surface . . . . .	95
36. SEM Micrographs of Large Spherical Particle . . . . .	97
37. Light Micrographs of Sphere Shown in Figure 36 . . . . .	98
38. SEM Micrograph of Small Spheres on Fracture Face of Inconel 625 . . . . .	100
39. High Magnification SEM Micrograph and Iron-K $\alpha$ Radiation Area Map of Spheres Shown in Figure 38 . . .	101
40. SEM Micrograph of Hollow Sphere. . . . .	102

## CHAPTER I

### INTRODUCTION AND HISTORICAL REVIEW

Flash welding is a resistance welding process which is used to produce high quality ring products and other welded parts at high production rates. Tubing, bar stock, forgings, and extrusions can be welded in shapes approximating the cross section of the finished product which results in large savings of expensive materials and in minimized subsequent machining costs. Also, little or no weld edge preparation is required (1, 2)\*. The weld is generally as strong as the base metal, and its ductility varies from 30-70 percent of the base material (3). The fatigue properties of flash welded joints, after the upset is removed, are generally equal to or better than those of joints produced by other welding processes (2). It is a versatile process in that materials from carbon steels to high alloy steels and from superalloys to refractory and reactive metals may be welded with this process. Also, many dissimilar metal joints are possible.

Flash welding is used in the fabrication of many products in the United States. One significant automotive application is in the production

---

\* Superscript numbers in parentheses refer to references entered in the List of References.

of wheel rims for cars , trucks and buses<sup>(1, 2)</sup> . Aircraft landing-gear and railroad rails are joined using flash welding<sup>(1, 2)</sup> . Fittings for petroleum industry drilling pipe are attached by flash welding<sup>(1)</sup> . The miter welds in window frames for the automotive and building industries are flash welded<sup>(1, 2)</sup> . Band-saw blades are flash welded into continuous loops<sup>(2)</sup> . Probably some of the greatest savings are gained by the use of the flash welding process in the welding of costly corrosion-resistant and high-temperature alloys for jet engine and missile component fabrication<sup>(1)</sup> .

As previously mentioned , flash welding is a resistance welding process . The workpiece or pieces are clamped in current-carrying fixtures called platens . One platen is movable and the other is stationary . The process is begun by advancing the movable platen until the workpieces are brought into light contact . As contact is made , current flow is initiated . This current is very high in amperage , and the voltage is low . Typical currents are given in terms of tens of thousands of amperes , and some machines are capable of producing over 65,000 amperes . Because the voltage is only about 4-10 volts , current flow occurs only where the interfaces touch . Since initially only a few random points are in contact , these short circuiting areas experience extreme levels of localized heat . Different contact areas are repeatedly raised to the melting point , exploded in a fuse-like action , and expelled from the interface as the movable platen is mechanically or hydraulically advanced . Eventually , the flashing action is continuous over the entire abutting surfaces . If the platen

advancement is correct, the heat generated by the flashing will raise a small region adjacent to the faying interface to the desired forging temperature within the plastic range. This usually takes from 1-60 seconds. Then the speed of the moving platen is suddenly increased so that the workpieces are forged together expelling the molten metal from the interface and upsetting a portion of the plastic metal thus forming the weld and an excess or flash on the part. This flash is normally removed by scarfing, grinding, or machining, and the parts are ready for use or other fabrication steps.

### Flash Welding Process Variables

The production of defect-free flash welded parts requires an understanding and control of many welding variables. All process variables may be classified as either flashing variables or upset variables. The flashing variables are the ones which determine the temperature distribution at the beginning of upset. The upset variables are the ones which affect the process from the beginning of upset until the welded assembly is removed from the welding machine.

Some of the more important flashing variables include the following<sup>(3)</sup>:

1. Preheat.
2. Initial extension - the initial distance between the clamping dies.



3. Flashing pattern or feed rate - the platen displacement as a function of time .
4. Flashing voltage .
5. Flashing burnoff - the material consumed during flashing .

Frequently several different combinations of flashing variables will yield approximately the same temperature distribution , but the optimum set is the one which requires the smallest flashing burnoff and the least time<sup>(3)</sup> .

A preheating cycle is sometimes used in the welding of heavy sections because the elevated temperature of the work interfaces permits easier starting and sustained flashing at a lower operating voltage<sup>(3)</sup> . Preheating can also reduce the flashing burnoff because the desired temperature distribution can be obtained in a shorter flashing time<sup>(2)</sup> . The preheating is accomplished by resistance heating ( $I^2R$ ) of the joint under pressure in the flash welder .

The initial extension will affect the temperature distribution and thus the size of the resulting plastic zone . Unequal extensions of the two workpieces may be used to equalize the heat balance in the two pieces if they are of different sizes , shapes and/or materials . A proper heat balance will ensure good upsetting of the workpieces<sup>(2)</sup> .

A good flashing pattern will allow continuous flashing and thereby yield the desired temperature distribution with the least flashing burnoff (2 , 3) .

Although it has been shown that the temperature distribution is not influenced by the flashing voltage, it is still a very important variable<sup>(4)</sup>. Riley<sup>(5)</sup> showed that the size of the craters formed on the flashing interfaces by the expelled molten material is minimized as the flashing voltage is decreased. The desirability of producing only small shallow craters during flashing will be covered in greater detail later in this report.

The following upset variables<sup>(3)</sup> must be controlled to produce optimum results:

1. Rate of closure.
2. Flashing current cut-off time.
3. Upset force.
4. Upset velocity and distance.
5. Upset current magnitude and duration.

The rate of closure must be fast enough to allow expulsion of the molten metal film from the weld joint before it solidifies and traps impurities on the faying surfaces. The flashing current cut-off time must be synchronized with the rate of closure to prevent undesirable cooling of the workpieces prior to upset.

The upset velocity must be fast enough to prevent solidification of the molten metal before it is expelled from the joint. The upset force and distance must be great enough to close all voids and to expel the molten metal and impurities from the workpiece cross sections<sup>(2)</sup>.

The upset current must counterbalance the heat loss so that the required upset force is not greatly increased. If this is the sole purpose for the upset current, it will terminate when the upset is complete. If a slower cooling rate is desired to prevent phase transformations or to reduce the magnitude of residual stresses, the upset current will terminate at some time after the completion of the weld<sup>(3)</sup>.

### Flash Weld Defects

Flash welding is normally a completely automated process possessing great reproducibility. However, defects in flash welded joints are encountered, normally during set-up, and must be eliminated or minimized in the finished part. Flash welding defects may be classified as to their origin as either mechanical or metallurgical defects<sup>(3)</sup>. A typical example of a mechanical defect is the inferior weld caused by misalignment of the workpieces in the welding machine. Metallurgical defects are usually associated with material defects or heterogeneities<sup>(3)</sup>. The most probable cause for rejection of flash welds is related to mechanical defects such as misalignment of the workpieces. These defects are easily found by visual inspection and can be corrected by simple machine adjustments. Metallurgical defects are much harder to find by nondestructive techniques because they are usually internal defects.

The various types of metallurgical flash weld defects are:

1. Cracking.

2. Intergranular oxidation.
3. Decarburization.
4. Voids.
5. Cast metal at bond line.
6. Oxides and other inclusions.
7. Flat spots.

The cause and/or prevention of the first six types of defects have been studied to some extent.

Cracking in flash welds can be divided into two categories depending upon the temperature of formation: (1) cold cracking and (2) hot cracking. Cold cracking can be caused by a combination of excessive upset and an improper temperature profile. Also excessive cooling rates in hardenable steels can cause cold cracking due to intolerable strains acting upon martensitic structures. This can be corrected by heat treating in a furnace immediately after welding or by postweld heat treating in the welding machine<sup>(2, 3)</sup>.

The most common form of hot cracking in flash welds occurs as microfissures in the heat-affected zone (HAZ) and is known as break-up. In stainless steels, Williams<sup>(6)</sup> found that the amount of break-up was a function of the ferrite content and strain in the HAZ. Low ferrite contents are detrimental because they reduce hot ductility. Summerfield and Apps<sup>(7)</sup> found that break-up occurred in two distinct regions. The first region was a network of rapidly etching areas in the form of branches which

extended from the weld line into the HAZ and contained increased amounts of chromium, manganese, molybdenum and decreased nickel. They found that this network was composed of cored austenite which contained higher ferrite concentrations than did the unaffected base metal. They theorized that this network was formed when molten metal from the flashing interface penetrated the grain boundaries in the HAZ. The extent of penetration was found to increase as the flashing time increased. The network was found to nearly disappear after a heat treatment at  $1050^{\circ}\text{C}$  for one hour. The second region was composed of intergranular cracks which were less predominant than originally thought. The reason for this was that the network, when heavily etched, appeared to be composed of cracks.

Probably the most common form of intergranular oxidation<sup>(2, 3)</sup> is known as die-burns. This defect is caused by localized overheating of the workpiece where it is held in the clamping die. Removal of the oxide film from the workpiece clamping surfaces by grinding will usually eliminate this problem. Improper workpiece extension can result in extreme temperatures away from the faying surfaces and as a result intergranular oxidation may occur there.

Another type of flash welding defect results from elemental redistribution. In carbon steel, this is manifested as decarburization. This defect appears as a bright band on the polished and etched surface of a flash welded steel specimen which is cut transverse to the weld line.

Forostovets and Dem'Yanchuk<sup>(8)</sup> studied this phenomenon in several heavy

section grade steels. They cut samples at oblique angles to the bright band in an effort to magnify its width. Their metallographic studies showed that the bright band could be divided into three sections: (1) center, (2) edge and (3) transition zone (between bright band and parent metal). The chemical concentrations in each region were determined by spectrographic analysis. They found that the composition of the metal at the center depended upon the welding conditions and varied greatly. The concentration of all elements exhibited a minimum just inside the edge of the bright band and a maximum in the transition zone near the edge of the bright band. This chemical heterogeneity affects the mechanical properties of the weld joint. In particular, the variation in carbon concentration greatly affects the hardness, ductility, and strength. The authors attributed the chemical heterogeneity to a redistribution of the alloying elements and impurities between the solid and molten metal present at the interface during flashing.

Another study also by Forostovets<sup>(9)</sup> showed that the bright band is ferritic only in mild steels and becomes mainly acicular and martensitic in steels with higher carbon and alloying element concentrations. Heat treatment at high temperatures was found capable of eliminating these bands.

Three types of defects (oxides and other inclusions, voids, and cast metal in the weld joint) are related by the fact that all three can usually be eliminated by parabolic platen advancement and/or greater

upset<sup>(2, 3)</sup>. As previously mentioned, craters are formed on the faying interfaces by the expulsion of molten metal during flashing. If the voltage is too high<sup>(5)</sup> or the platen speed is held constant<sup>(10, 11, 12)</sup>, violent flashing occurs and deep craters are formed. Johnson's work<sup>(10)</sup> indicated that there is a minimum upset length for complete elimination of these weld defects. An upset length less than this results in numerous defects because the craters cannot be totally removed. Kilger<sup>(13)</sup> found oxidized craters on the fracture surfaces of specimens exhibiting low fatigue strength. He attributed this to insufficient upset. Hess and Muller<sup>(14)</sup> found that parabolic platen speed would eliminate oxide inclusions at the weld line while increased upset would minimize or eliminate cast metal in the weld joint.

The cause and prevention of flat spots is not very well understood. In fact, the term itself is vague and is often used to describe several different features. These fracture features may be the result of a number of metallurgical phenomena having inherently different mechanisms. The smooth, irregular shaped areas indicated by arrows in Figure 1 are flat spots on the fracture surface of a flash welded Hastelloy X sample. Figure 2 is a 100X SEM micrograph which shows the variation in topography on the fracture surface. A plateau region can be seen which contains three relatively flat areas (A, B, and C) which are separated by rougher, more ductile areas. At higher magnification (Figure 3, 300X), it is apparent that for this alloy the flat spots are relatively featureless. However, in



Figure 1. Macrograph of the mating fracture surfaces from a flash welded Hastelloy X sample. The arrows indicate the presence of flat spots. 1.5X



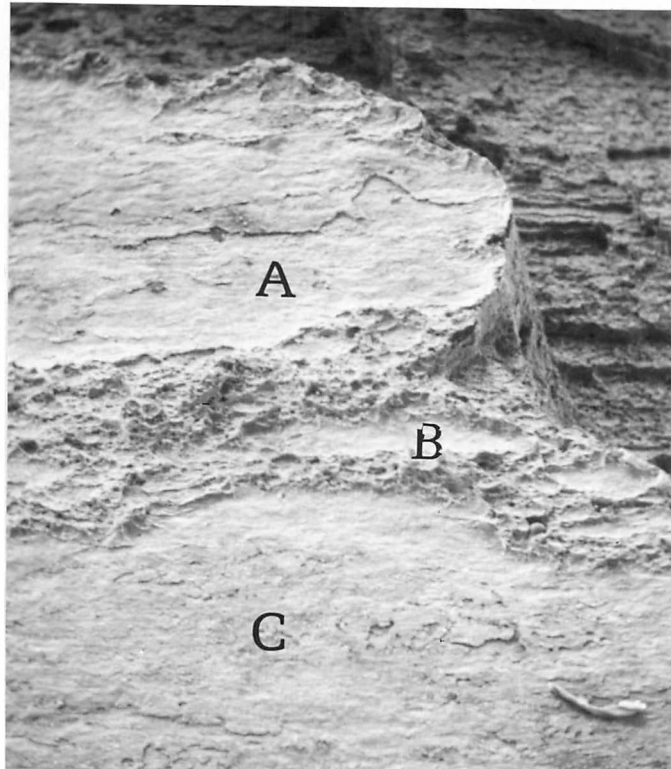


Figure 2. Scanning electron micrograph of some flat areas on the fracture surface of a flash welded Hastelloy X sample. 100X



Figure 3. Higher magnification scanning electron micrograph of flat areas seen in Figure 2. 300X

other areas and in other alloys, numerous inclusions and very small dimples appear. This is in contrast to the rougher, larger dimpled area shown separating these flat areas. Barrett's metallographic investigation (15) of some flash welds made in large diameter, heavy wall alloy steel tubes revealed flat spots on fracture surfaces of numerous samples. He theorized that they were caused by oxidized craters on the faying interfaces which were not removed during upset. He stated that these oxides were complex and included silicates and aluminates. He did not mention his analytical technique. It was stated that higher chromium steels were more prone to contain chromium oxides and the resulting flat spots. In an effort to prevent the formation of these oxides, Barrett introduced shielding gas into the flashing region by directing the flow through one of the tubes to be welded. He found that the number and size of flat spots were reduced by the addition of the gas atmosphere, and that hydrogen was more effective than city gas. It appears that when a featureless flat spot occurs it probably is the result of flattened oxidized craters. This has been documented in this study also.

An investigation by Nippes, et al<sup>(16)</sup>, which included microhardness tests and metallographic studies, showed that the flat spots in steels are usually surrounded by high-carbon martensite. Faulkner and Shaw<sup>(11)</sup> observed fine-grained, lenticular defects in metallographic samples made from flash welded railroad rails. Examination showed that the decarburized region at the weld line split and surrounded the lenticular defects which

were high in carbon content and hardness. These defects were also enriched in sulphur and phosphorus. When the platen speed was increased in a parabolic fashion (constant acceleration), the defects no longer appeared in metallographic specimens. They believed that these defects were caused by excessively large craters which were not totally removed during upset. They theorized that when the specimens were fractured these defects yielded flat spots. Gordon and Young<sup>(17)</sup> observed that flat spots were more numerous in thick wall steel tubes containing chromium and that the use of inert gas reduced their occurrence. They also showed a photograph of a fractured weld sample which exhibited a ridged effect (a series of parallel, narrow flat streaks) which they attributed to a concentration of carbides in the base material.

Sullivan and Savage<sup>(18)</sup> studied the effect of varying the electronic phase control during flashing upon the occurrence of flat spots. They found that the probability of flat spots increased when a phase control setting of less than 100 percent was utilized. They attribute this increase to entrapped liquid pools of modified composition which are not expelled from the cross section. The pools originate because the greater current surges (associated with reduced phase control settings) cause much larger interface craters which are more difficult to remove during upset. They theorized that the pools were modified by solute diffusion from the underlying base metal and by reaction with gases in the ambient atmosphere.

The resulting solidified material exhibits reduced ductility and appears as a flat spot when the specimen is fractured.

Although the above theories have been suggested for the cause of flat spots , none has been universally accepted. A better understanding of this phenomenon is necessary because the presence of flat spots reduces the ductility of welded joints. The problem is compounded by the fact that a satisfactory nondestructive test for detection of flat spots has not been found.

#### Object

The purpose of this investigation is to determine the nature and morphology of weld defects on the fracture surfaces of flash welded high temperature , high strength alloys .

## CHAPTER II

### MATERIALS AND PROCEDURES

#### Materials

Five iron-nickel base superalloys were investigated in this study. They are: (1) Hastelloy X, (2) Inconel 625, (3) Alloy 718, (4) N-155, and (5) Waspaloy. Flash welded specimens from each alloy were supplied by American Welding and Manufacturing. The composition of these iron-nickel base alloys is given in Table I<sup>(19)</sup>.

Hastelloy X is a nickel-base alloy which has good strength and oxidation resistance up to 2200<sup>o</sup> F. Its strength is obtained from carbide precipitation and the solid solution effect of columbium and molybdenum in the primarily nickel matrix<sup>(20, 21)</sup>. This alloy is used in industrial furnace parts in addition to parts for aircraft turbine engines.

N-155 is an iron-nickel-chromium-cobalt alloy which is recommended for use in applications involving high stresses at temperatures up to 1500<sup>o</sup> F and moderate stresses up to 2000<sup>o</sup> F<sup>(22)</sup>. Strengthening is produced by the solid solution of columbium, molybdenum, and tungsten in the nickel-chromium-iron matrix and by the precipitation of complex carbides<sup>(20)</sup>. Turbine blades and sheet metal parts are made from this alloy<sup>(22)</sup>.

TABLE I

THE COMPOSITION OF IRON-NICKEL BASE SUPERALLOYS USED IN THIS INVESTIGATION

Alloy	Ni	Cr	Co	Mo	Fe	C	Others
Inconel 625	Bal	22.5		9.0	5.0 max	0.05	3.6 Cb, 0.2 Mn, 0.3 Si
Alloy 718	Bal	19.0		3.0	18.0 max	0.04	5.0 Cb, 0.6 Al, 0.8 Ti, 0.2 Mn, 0.2 Si, 0.1 Cu
Hastelloy X	Bal	22.0	1.5	9.0	18.5	0.10	0.5 Mn, 0.5 Si, 0.6 W
Waspaloy	Bal	19.5	13.5	4.3	2.0 max	0.07	3.0 Ti, 1.4 Al, 0.09 Zr, 0.006 B
N-155	20	21.0	20.0	3.0	Bal	0.15	2.5 W, 0.15 N, 1.0 Cb, 1.5 Mn, 0.5 Si

Inconel 625<sup>(23)</sup> is basically a nickel-chromium-molybdenum alloy which has excellent resistance to corrosion and oxidation. In addition, it has good strength and toughness at temperatures ranging from cryogenic to 2000° F. Strength is obtained by the solid solution effect of molybdenum and columbium in the nickel-chromium matrix<sup>(21, 22)</sup>. Carbides ( $MC$ ,  $M_6C$  or  $M_{23}C_6$ ) and nitrides may be present in the microstructure, but their contribution to material strength is insignificant. This versatile material is used for jet engine components, chemical processing construction and specialized sea water equipment.

Alloy 718 and Waspaloy are two nickel-base alloys which depend upon the precipitation of gamma prime for their strength. This phase and its strengthening effect are retained at high service temperatures. Alloy 718<sup>(24)</sup> is a high strength, corrosion-resistant material which is used at temperatures from -423° F to 1300° F. It is strengthened by the coherent  $Ni_3$  (Cb, Al, Ti) phase<sup>(24)</sup>. Waspaloy is also a high strength, corrosion-resistant alloy which is primarily strengthened by the precipitation of  $Ni_3$  (Al, Ti) during aging<sup>(25)</sup>. Both alloys are used in making aircraft turbine engine parts while only Alloy 718 is found in cryogenic applications<sup>(24)</sup>.

### Equipment

Use of the scanning electron microscope (SEM) has increased tremendously during the last five or six years. This surge of interest is due to the SEM's versatility and the ease of both operation and interpretation



of results. The SEM has bridged the gap between the optical and transmission microscopes in terms of magnification and resolution. The SEM is the superior microscope for the study of fracture surfaces due to its great depth of focus and wide magnification range (shown in Table II). In addition, practically no specimen preparation is required since the surfaces are examined directly thereby eliminating the possibility of replica artifacts.

The scanning electron microscope shown in Figure 4 utilizes a focused electron beam which is scanned on the specimen surface in a two-dimensional raster<sup>(26, 27, 28)</sup>. Interaction of the electron beam with the specimen produces the various signals shown in Figure 5. The secondary or back-scattered electrons are collected in a scintillation counter whose amplified signal is fed into a cathode ray tube which is scanned synchronously with the electron beam. The lower energy secondary electrons must be accelerated into the counter by a positively-charged grid. The result is a realistic image on the cathode ray tube which has a three-dimensional appearance due to secondary emission characteristics and the SEM's large depth of field. The image contrast<sup>(26, 27)</sup> is produced by differences in surface topography, atomic number, and secondary emission coefficient. Ridges or peaks on the specimen appear bright because the locally high surface area allows the electrons to easily escape. Low atomic number elements appear dark because of the ready absorption of electrons and small backscatter. Low work-function regions appear

TABLE II  
CHARACTERISTICS OF SEVERAL TYPES OF MICROSCOPES

Microscope	Magnification Range	Resolution	Depth of Focus
Optical	15-1500X up to 3000X	1000 Å with ultra	250 um at 15X
	with quartz optics and ultra violet radiation	violet radiation	0.08 um at 1200X
Scanning Electron	20-50,000X	100 Å to 10,000X	1000 um at 100X 10 um at 10,000X
Transmission Electron	200-300,000X	5 Å at 500,000X	500 um at 4000X 0.2 um at 500,000X

Source: J. Temple Black, "SEM: Scanning Electron Microscope," Photographic Applications in Science, Technology, and Medicine, 4(16), pp. 29-44, 1970.

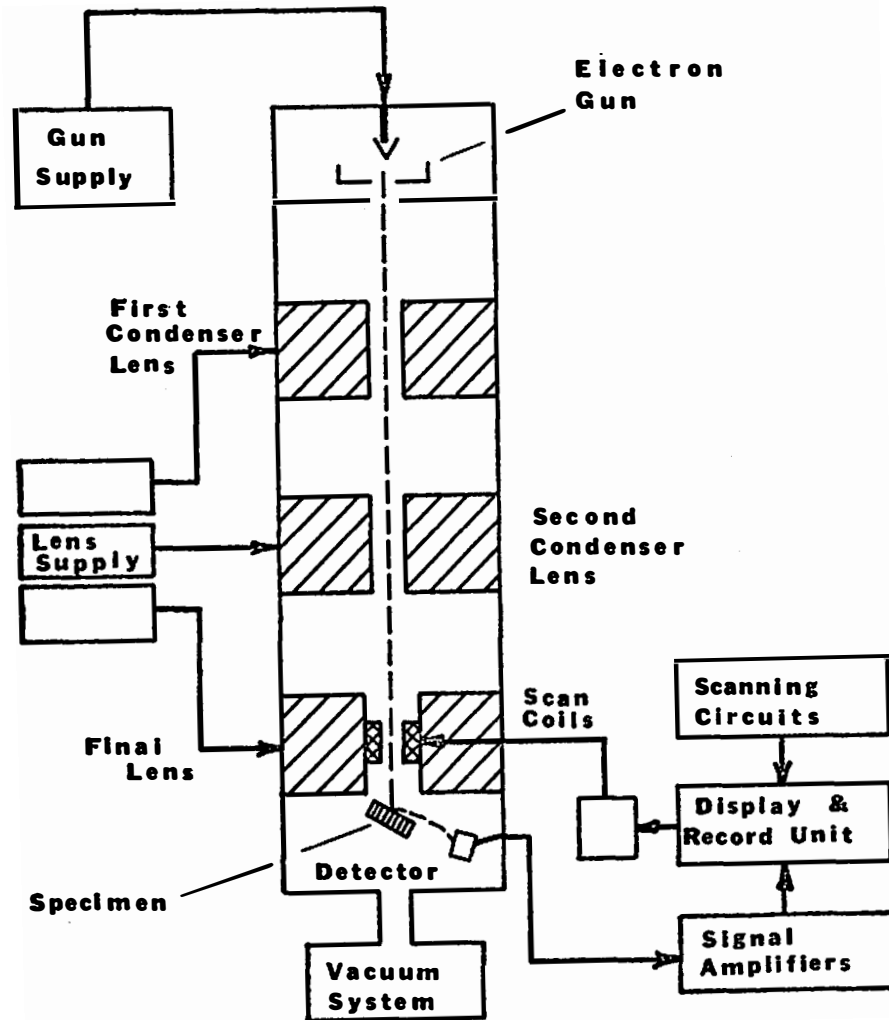


Figure 4. Schematic diagram of scanning electron microscope.

Source: R. F. Brandon (ed.), "Electronic Imaging Techniques," Techniques of Metals Research, Vol. II, Interscience Publishers, New York, pp. 89-91, 1968.

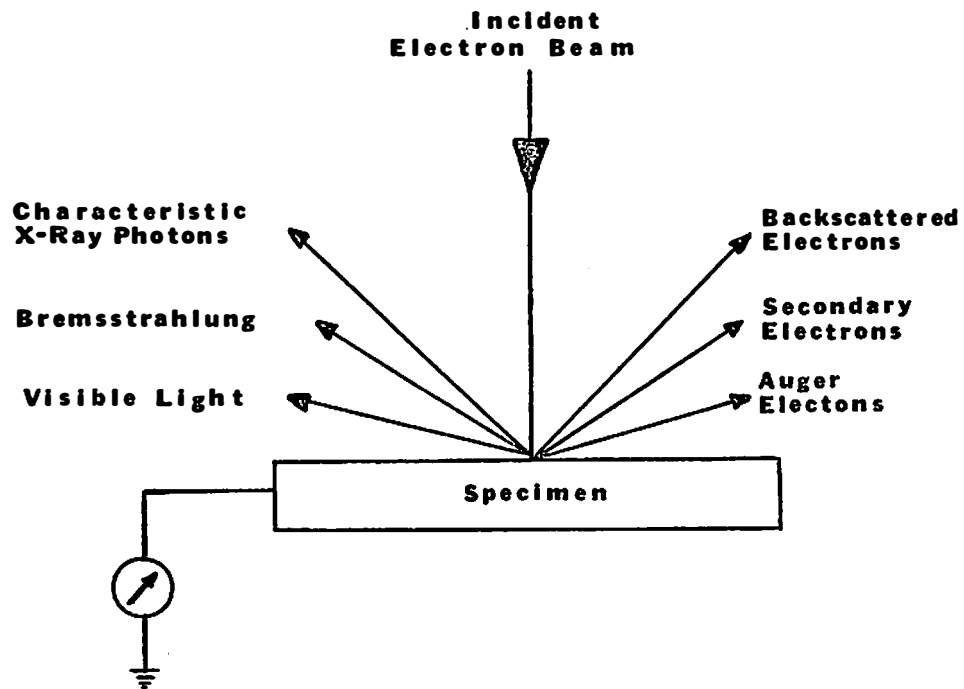


Figure 5. Signals generated in the scanning electron microscope.

Source: "Modern X-Ray Analysis II," EDAX International, Prairie View, Illinois, 1972.

bright because of the associated high secondary electron emission coefficient.

The scanning electron microscope becomes a much more powerful tool with the addition of an auxiliary energy dispersive (ED) x-ray analyzer. This device can be used to determine the composition of phases or features which appear on the specimen surface by recording the energy of the characteristic x-rays, shown in Figure 5, which are produced when the electron beam interacts with the desired region. These x-rays are collected by a lithium-doped silicon detector which produces photoelectrons in proportion to the energy of the incident x-ray<sup>(29, 30)</sup>. The charge produced by the detector is amplified and sent to a multichannel analyzer where the magnitude of the pulse (which is proportional to the intensity of the incident x-ray) corresponds to a location in the energy spectrum<sup>(30)</sup>. Each incident x-ray produces a pulse which is added to the appropriate location within the energy spectrum. Energy dispersive analysis is very rapid because a high efficiency detector is used and because the entire energy spectrum can be simultaneously analyzed with only one orientation of the specimen<sup>(29, 31)</sup>. In contrast, wavelength dispersive (WD) techniques require numerous precise orientations of the crystal for complete analysis. Another advantage of ED techniques is that analysis of specimens having rough surfaces is possible although true quantitative analysis is not<sup>(31)</sup>. Analysis of these specimens is very difficult by WD techniques because of the geometrical requirements for diffraction. For this reason

specimens analyzed in an electron probe microanalyzer are flat and mounted in a fixed geometry so that the necessary corrections can be made for absorption, atomic number, and characteristic and continuum fluorescence<sup>(32)</sup>. Use of these correction factors permits quantitative analysis of flat specimens in both the electron probe (WD) and scanning electron microscope (ED). The principal limitation of the ED x-ray analyzer is its inability to resolve energies of less than 1 Kev. This difficulty is due primarily to the thin beryllium window which protects the detector from contamination<sup>(31, 32)</sup>.

### Experimental Technique

Longitudinal and transverse base metal specimens were cut from each alloy using an abrasive wheel. These specimens were mounted in epoxy and rough polished using silicon carbide papers. This was followed by hand polishing on 6  $\mu$  diamond paste. Final polishing was performed by hand using 1  $\mu$  alumina, liquid detergent and water. All specimens were heated in running tap water before etching with aqua regia (80 percent HCl + 20 percent HNO<sub>3</sub>). Metallographic examination was performed on a bench metallograph.

Welded specimens were notched at the weld interfaces with an abrasive wheel and then slowly bent to failure in a three point bending fixture. The fracture surfaces were examined and photographically recorded using the AMR Model 900 scanning electron microscope. Elemental

analysis of the distinctive fracture features (e.g. flat spots) was accomplished using an Ortec energy dispersive x-ray system (Model 6200 multi-channel analyzer) which is an auxiliary part of the SEM. Semi-quantitative x-ray analysis was performed using the spot analysis technique. Tantalum foil was used to prevent influence of the aluminum specimen holder. Enlarged apertures and a large number of total counts (200,000) yielded rapid and comparative data.

When the fracture surface analyses were completely documented, metallographic sections were prepared by welding wire markers adjacent to features to be investigated optically. The samples were then nickel plated (to improve specimen edge retention during polishing), cut, and mounted. Soft-fired alumina powder was added to the epoxy to further aid in retaining the specimen edges. The specimens were ground until the wire markers were observed and then polished in the normal manner. A final polish on .5  $\mu$  diamond paste in a Syntron vibratory polishing machine was utilized in addition to the previously mentioned polishing procedure. The specimens were then etched and examined. Selected regions were analyzed in the SEM using the energy dispersive x-ray attachment. The elemental distributions were recorded using both photography and counting methods.

## CHAPTER III

### RESULTS AND DISCUSSION

The effect of the flash welding process variables on weld ductility has constituted the bulk of the previous investigations. While these investigations were often able to produce welds with adequate ductility by altering process parameters, occasions arose where the normal techniques failed to produce the desired results. Thus, it appeared that the material variables were quite often as important as the process variables.

The early investigations lacked the sophisticated metallurgical tools to adequately document the influence of material variables on weld ductility. Only recently has the ability to examine bulk fracture surfaces been available to the welding engineer and metallurgist. This recent development has been brought about by the advent of the SEM and its ancillary elemental analysis capability. Through the use of this instrument, rapid and definitive conclusions can be reached regarding fracture mode, macroscopic and microscopic ductility, and the role of inclusions or second phase particles on the nature and morphology of flat spots in flash welds. Thus, the emphasis in this study has been on the material-related phenomena which have not been adequately documented in previous investigations.

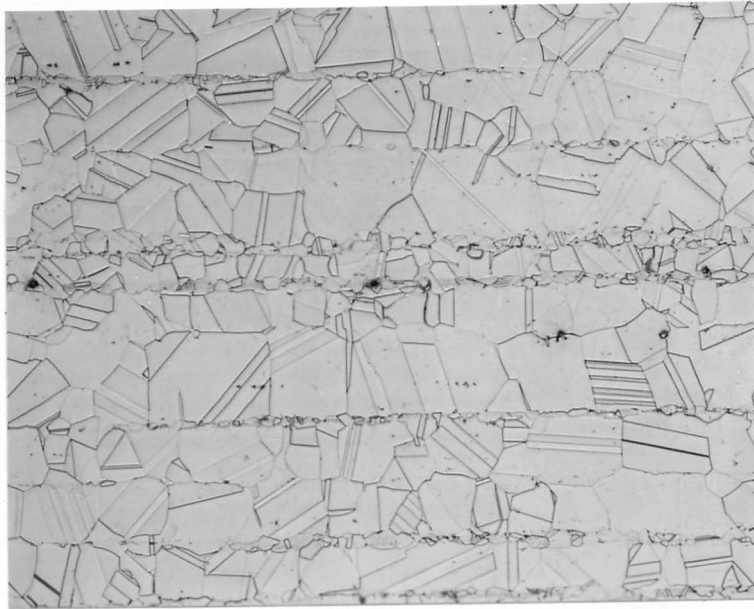


## Materials

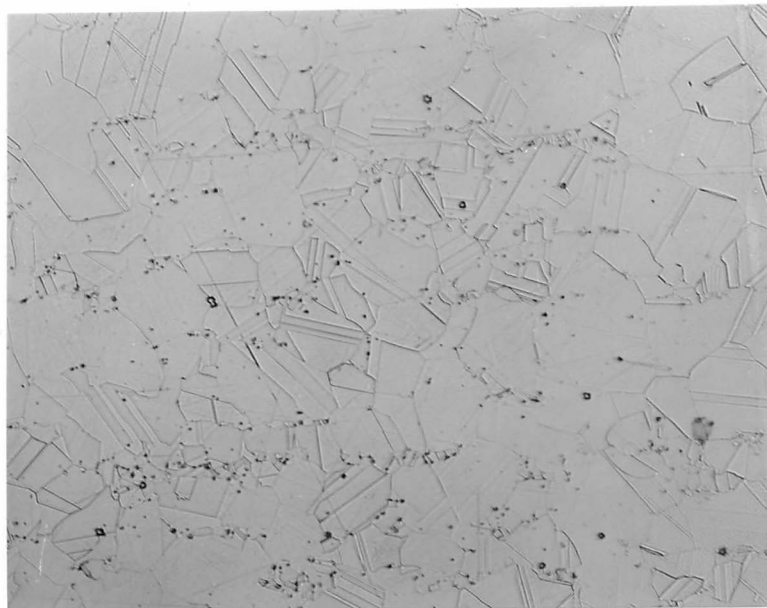
General. Most flash welding applications involve the use of wrought products. The origin of most wrought products is an ingot derived from a melt. Inherent in the original solidification process is alloy segregation and grain size and shape variation. During subsequent mechanical treatments to reduce the ingot to the desired configuration, the original segregate pattern is seldom completely eliminated. It is, however, normally altered in accordance with the total percentage of thickness reduction and direction of material flow during the deformation process. For example, bar stock will exhibit a banded microstructure which is elongated primarily parallel to the major axis of the bar. This banded microstructure is inherited from the original solidification process and consists of alloy segregation and/or inclusion and second-phase particle distributions.

Depending upon the alloy, its transformation and recrystallization behavior, and the mechanical/thermal treatment, grain size variation may be evident. Precipitate morphology may also follow the banding pattern. For simple geometries such as bars or plates, the banded microstructural pattern is likewise relatively simple and predictable. The extent of transverse banding is also dependent on crossrolling and the extent of reduction.

Materials used in this study. The base materials used in this study exhibited the general type of elongated and banded microstructure which was discussed above. Figure 6 shows the microstructure of



(A) Longitudinal section. 100X



(B) Transverse section. 100X

Figure 6. Micrographs of banding in Waspaloy base material.

longitudinal and transverse metallographic sections cut from the Waspaloy base material used in this study. Alternating bands of large and small grained regions are evident in Figure 6A. The small grains were caused by the high particle densities in the bands which pinned the grain boundaries during the thermal-mechanical treatments. Figure 6B shows the flattened particle bands as they appear in a transverse section. The relationship between particle density and grain size is more evident in this section. Waspaloy was the only alloy in this study that exhibited such a large variation in grain size.

The Hastelloy X base material also contained extreme banding as seen in the longitudinal metallographic section shown in Figure 7. The microstructure is composed of alternating bands of light and dark regions. Figure 8 shows that the darker etching regions consist of a finer grain size, and the grain boundaries are filled with second-phase particles. The particles are not evident in the lighter etching regions, and the grain size is larger.

Figure 9 is a micrograph of a longitudinal section from the Inconel 718 base material used in this investigation. The microstructure shows little banding other than particle stringers. The grain size shows random variations. This microstructure is also closely representative of the N-155 and Inconel 625 base materials which were also investigated.

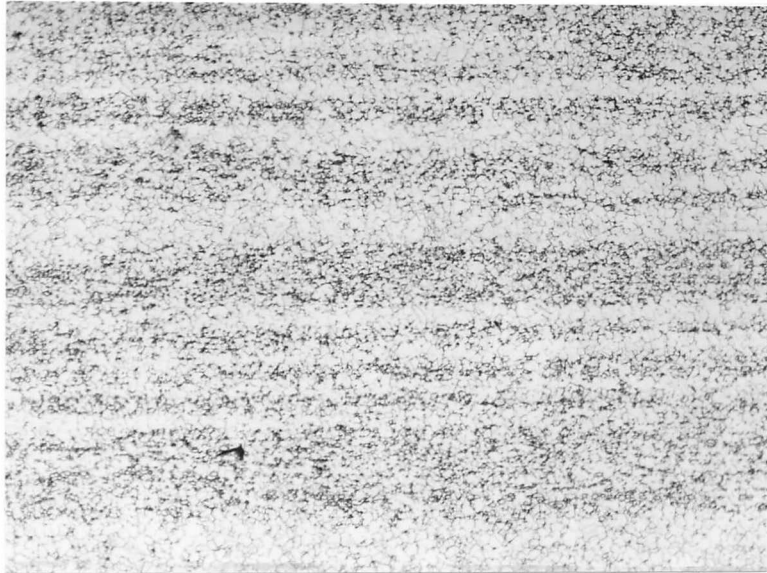


Figure 7. Micrograph of longitudinal section from Hastelloy X base material. 100X



(A) Light band. 500X



(B) Dark band. 500X

Figure 8. High magnification micrographs of bands from Figure 7.

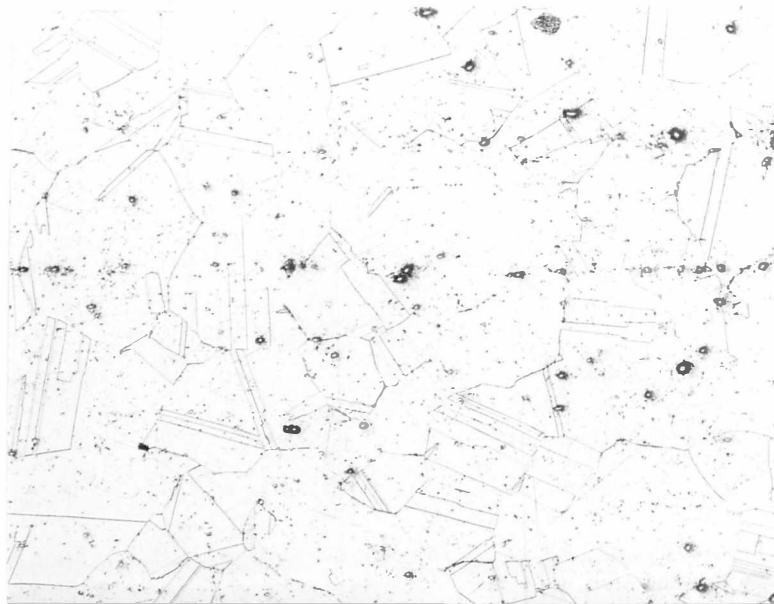


Figure 9. Longitudinal microstructure of Inconel 718 which is also representative of N-155 and Inconel 625. 100X

### Effect of Microstructure on Fracture Propagation

Due to ingotism and its subsequent alteration by mechanical working, properties in the short transverse direction (through the plate thickness) are known to be inferior to those in the other two orthogonal directions. This is also manifest in the well-known welding related problem called lamellar tearing. Lamellar tearing normally occurs under a weld bead where shrinkage strains oriented perpendicular to the plate surface cause separation along the microstructural banding. The separations are the result of voids which nucleate at the interface between nonmetallic inclusions and the matrix<sup>(33, 34)</sup>. This nucleation of voids results in a series of "dimples" on the fracture interface. The inclusion spacing within the microstructural bands is such that a relatively small amount of total strain is required to cause linking of the dimples and thus a complete separation or tear. This type of fracture surface appears to be macroscopically flat indicating low ductility. As will be noted later, this low ductility fracture mode is often evident in flash welds for almost identical reasons.

Actually, the number of possible fracture modes in the alloys studied is quite limited. There are only three major modes of fracture<sup>(35)</sup>: (1) cleavage fracture, (2) plastic fracture, and (3) intercrystalline fracture. Cleavage fracture, which occurs by separation normal to crystallographic planes of high atomic density, is not very likely in these alloys because they are face-centered cubic in nature. Cleavage fracture in face-centered cubic alloys is a rare occurrence. Plastic fracture can occur either by

uninterrupted plastic deformation or by formation and coalescence of microvoids. Fracture by uninterrupted plastic deformation (also known as "rupture") occurs as continuous necking until the load carrying cross section approaches zero before failure. This results in a fracture surface which resembles a chisel edge for sheet material and a point for round bar stock.

Most ductile fractures do not approach the nearly 100 percent reduction in area exhibited by materials which fracture by "rupture". The less ductile fractures, which are the most common, occur by formation and coalescence of microvoids. Coalescence is actually the link-up of the microvoids by microscopic necking which occurs along the microvoid intersections. When link-up is complete, fracture occurs. Thus the voids yield dimples on the fracture faces. Intercrystalline fracture is the separation of crystals from each other along grain boundaries. Often this type of fracture is caused by brittle grain boundary films or by a large population of grain boundary precipitates<sup>(36)</sup>. Thus the most likely mode of failure in the iron-nickel base superalloys investigated in this work is the formation and coalescence of microvoids.

Confusion often results when fracture surfaces are classified by macroscopic examination as either ductile or brittle. The confusion occurs because many fracture surfaces which do not exhibit detectable macroscopic deformation have, in fact, failed by the formation and coalescence



of microvoids. As previously described, this is a localized plastic rupture process.

Passoja<sup>(37)</sup> developed a theoretical model for predicting the impact energy of metals containing nondeformable particles. His model related the energy required to form two fracture faces to the interparticle spacing in a two-dimensional material system. He assumed that voids nucleated at the particles and that the particle-matrix interfacial energy was low. The equation which he developed to calculate the theoretical impact energy for steels fractured on the upper shelf is:

$$CVN = 2.32 \bar{L}^{2.0}$$

where

CVN = the impact strength in foot-pounds.

$\bar{L}$  = the mean linear intercept dimple size in microns (e.g. interparticle spacing).

This equation was developed using material parameters for mild steel. Substitution of material parameters for other alloys will change the value of the coefficient and exponent but not the general form of the equation.

The impact energy is directly related to the energy necessary to create two surfaces and is found to be proportional to the square of the mean dimple size. Thus, small dimples indicate low energy absorption during fracture. This result indicates that any area of a fracture face which exhibits smaller dimples than its surroundings required less energy

to fracture. The total strain to fracture varies in a like manner because the smaller the interparticle spacing the lower the total strain to failure. Widgery<sup>(38)</sup> has demonstrated this in his crack-opening displacement (COD) work with steels. He showed that the fracture strain decreased as the particle volume fraction increased.

The studies by Passoja and Widgery are really complementary. Passoja worked from fracture surfaces on which he could record both the number and the size of particles involved in the actual fracture while Widgery used polished and etched cross sections to determine particle volume fraction. Thus, Widgery included all particles in his analysis while Passoja included only those involved in the fracture process. It can be concluded from these investigations that the total fracture strain is lowered as either interparticle spacing decreases or particle volume fraction increases. These phenomena are synergistic and therefore normally occur simultaneously.

If the fracture strain is decreased, the total amount of plastic flow to cause fracture is likewise reduced. Thus, areas along the fracture path with large particle populations will be areas which exhibit flat, low ductility fracture.

When the workpieces are upset during flash welding, the banded microstructure of the base material is forced to turn outward at the weld interface as shown schematically in Figure 10. In fact, some of the bands become almost parallel to the weld interface. When this happens, the

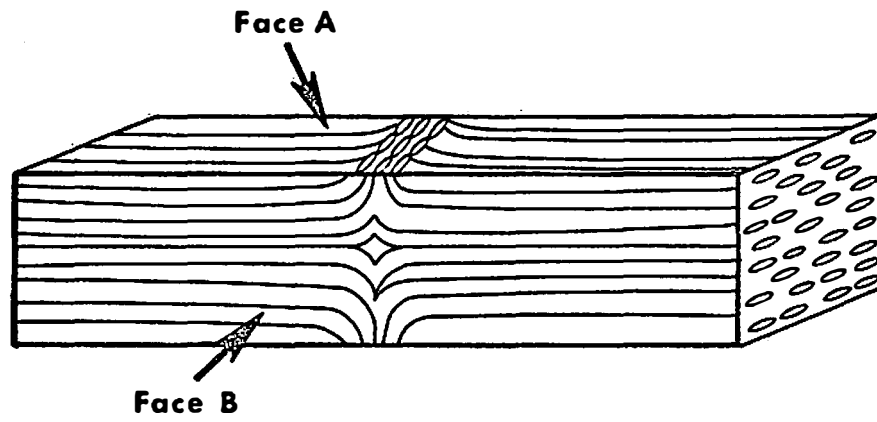
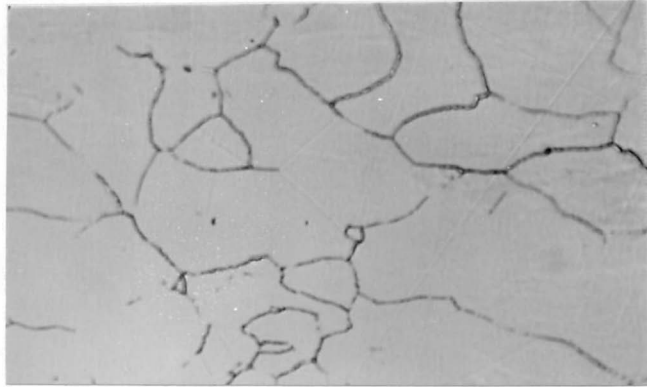


Figure 10. Schematic diagram of flash weld.

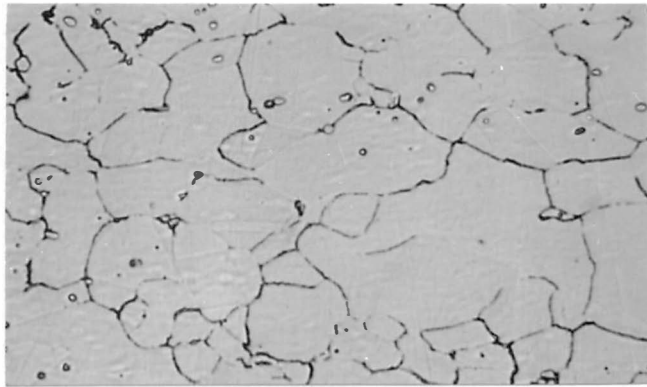
short transverse properties become, in essence, longitudinal properties at the weld interface.

In addition to the mechanical treatments received during the flash welding, the workpieces also experienced a thermal cycle which altered the microstructure near the weld interface. Recrystallization and grain growth may occur within the heat-affected-zone (HAZ). In addition, dissolution of second-phase particles may occur. Figure 11 shows the microstructure of Hastelloy X at three different distances from the weld interface. The disappearance of the carbides as the weld interface is approached is the result of dissolution due to thermal cycling. In some instances, reprecipitation of the dissolved particles may also be observed. If the thermal cycle is rapid enough, constitutional liquation may occur in some alloys. Figure 12 shows evidence of constitutional liquation in flash welded Hastelloy X<sup>(39)</sup>. Note the eutectic appearing structure and wetting of the grain boundaries. The cracks located within the liquated region indicate that this structure is brittle and may lead to premature fracture.

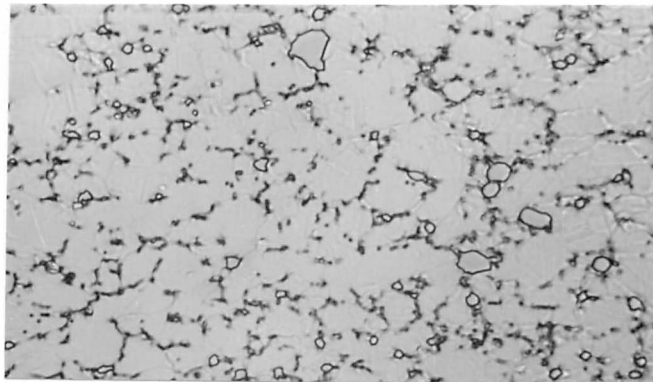
The integrity of flash welds is evaluated by subjecting the completed joint to a slow bend test using three point loading. This test yields qualitative ductility data. The specimen is notched at the weld interface and when subjected to three-point loading the specimen begins to fracture at the root of the notch. When the specimen has completely fractured, the fracture faces are examined for flat spots, oxides, and other deleterious features which indicate reduced ductility and therefore reduced formability



(A) .005 inch. 750X



(B) .050 inch. 750X



(C) .150 inch. 750X

Figure 11. Carbide population at various distances from the weld interface.

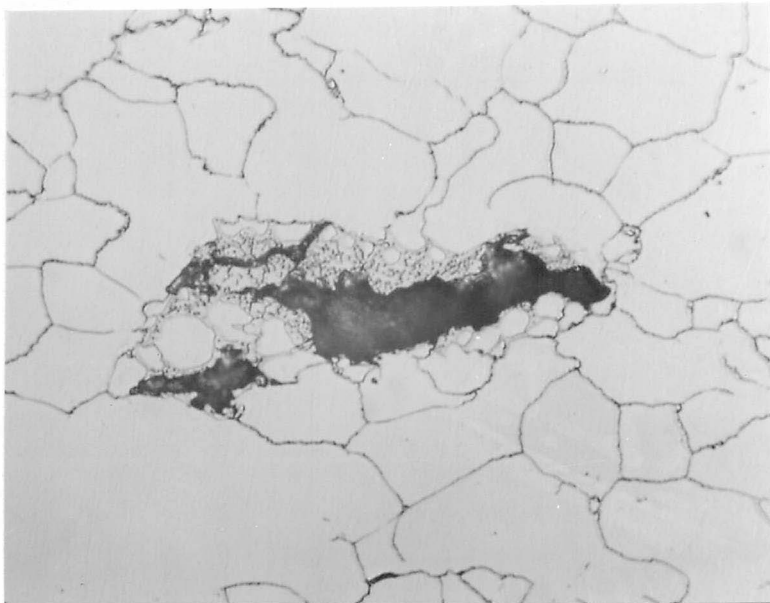
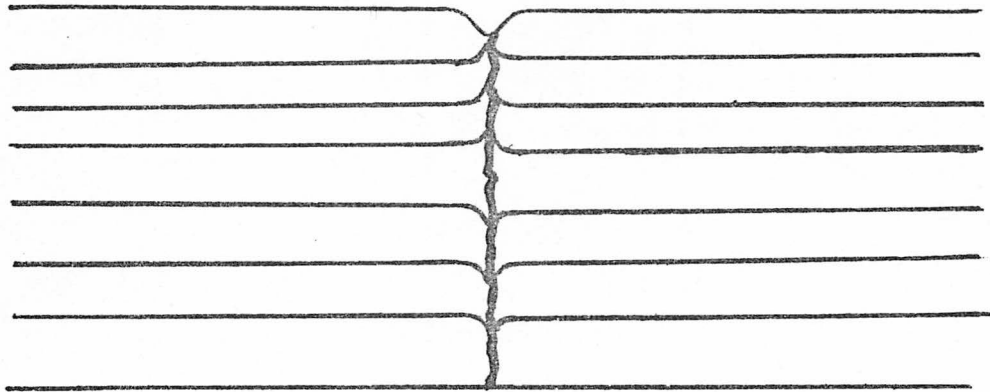


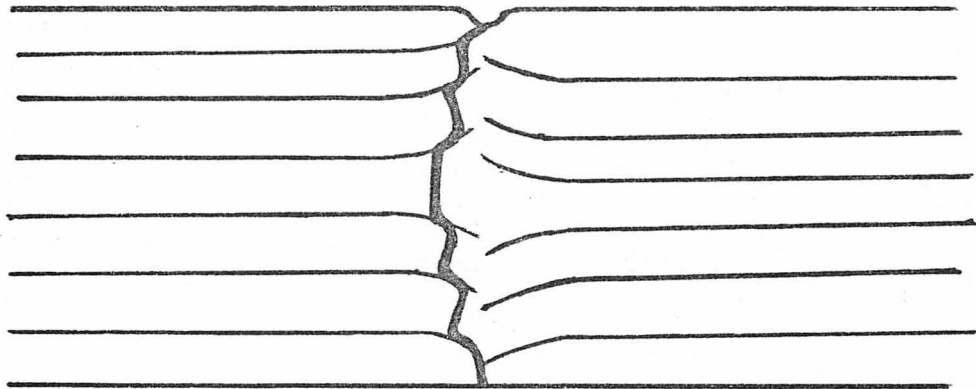
Figure 12. Constitutional liquation in flash welded Hastelloy X specimen. 750X

The phenomena described in previous discussions concerning banded microstructure, lamellar tearing, and deformation of the microstructure during welding can be used to predict fracture paths for slow bend specimens. The orientation between the banded microstructure and the crack initiation notch will influence the fracture path. If the weld joint is significantly upset during welding, the banded structure will be oriented approximately parallel to the weld interface. First assume that the weld is notched at the weld interface in face A, Figure 10, page 38. The fracture will progress from the root of the notch along the weld interface. If the microstructural bands contain many particles with a small interparticle spacing, fracture will progress by void coalescence along the bands with little total strain. Thus, the weld will exhibit low ductility. This is shown schematically in Figure 13A. A similar fracture path would be followed if a brittle oxide film were present at the weld interface.

If the weld joint is properly upset, the deformed banded microstructure will appear similar to that shown schematically in Figure 13B. In this case, a crack which initiates from a notch in face A again propagates along a path of least resistance. This path is usually along the curved and banded structure for the same reasons stated above. As the propagating crack becomes almost parallel to the principal stress, it stops and then crosses the more ductile matrix regions between the inclusion/segregate bands. When the propagating crack reaches another favorably



(A) Overly upset



(B) Proper upset

Figure 13. Effect of flash welding upset upon the fracture path for slow bend specimens having banded microstructures.



oriented band, the process is repeated resulting in a streaked or shingled fracture appearance. A streak is a long, narrow fracture feature in which the ductility is relatively low, and, thus, the surface is relatively flat. The streaks are separated by rougher and more ductile regions. The shingled appearance results from wider bands of inclusions which fracture for only a short distance before the crack changes direction and propagates to the next inclusion band. The process continues in this manner and interconnects many particle bands to form the characteristic shingled or stair-step appearance. Thus, the shingled appearance indicates a series of interconnected low ductility regions which exhibit a more equiaxed aspect ratio than streaks. These features will be more adequately discussed later.

The influence of the orientation between the deformed banded microstructure and the crack propagation direction can be revealed by comparing the fracture originating at the weld notch in face B with the above discussed fracture which initiated from a weld notch in face A. When the crack initiates along the notch, the crack front is presented with a microstructural variation which differs from point to point. This variation is symmetrical about the midplane of the specimen. The structure which is intersected by the propagating crack remains essentially similar as a function of propagation depth at the same location along the crack front.

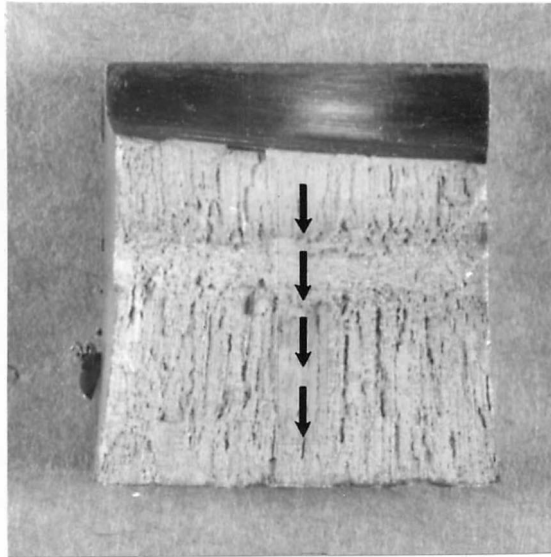
Since the orientation between the deformed and banded microstructure and the propagating crack is different depending on which of the two

faces (A or B) the fracture is initiated on, different fracture paths will be followed. Therefore, the fracture faces will differ in appearance as seen in Figure 14. Thus, the fracture appearance of the same structure is strongly dependent on fracture propagating direction.

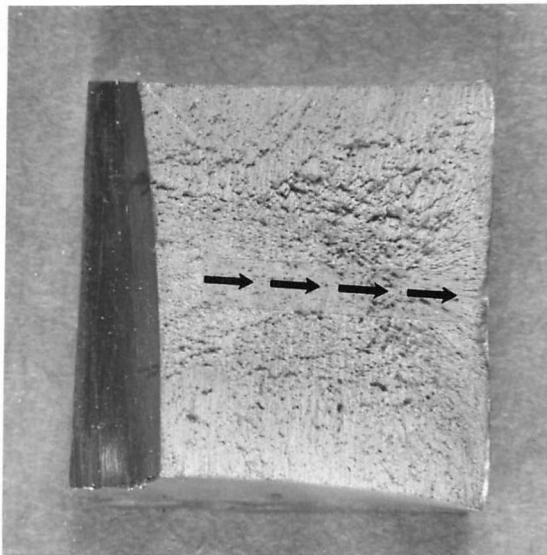
The materials welded in this study did not have simple cross sectional shapes such as round, square, or rectangular bar stock. In contrast, these materials took the form of complex configurations such as those used in the aerospace industry. By utilizing these complex configurations which approximate the cross sections of the final product, large savings can be realized in material and machining costs. The banded microstructures of these complex configurations will yield rather complicated deformation structures when upset during flash welding. Thus, many different and changing orientations between the propagating crack and banded microstructure will be encountered as the fracture progresses through these specimens. As a result, the fracture faces can be expected to exhibit a rather complicated appearance which varies from one point to the next.

#### Macroscopic Examination of Fracture Surfaces

Discussion of the specific fracture surface characteristics will be more meaningful if some definitions are first described. A flat spot is an irregularly shaped, macroscopically featureless region on a flash weld fracture surface whose length and width are of the same order of magnitude.



(A) Notch orientation A



(B) Notch orientation B

Figure 14. Effect of fracture propagation direction upon fracture face appearance.

Although some of the literature differentiates between flat spots and penetrators, this study will not since a penetrator is nothing more than a flat spot which extends to the surface of the joint.

Figure 15 shows the fracture faces of different flash welded joints made in Waspaloy. The flash weld fracture B exhibits a fine ductile appearance. The perimeter of the lower and right-hand sides is slightly streaked. In contrast the fracture surface appearance of the upper bar is very heterogeneous. Flat spots (indicated by arrows) can be seen on the left side and the upper right-hand corner. These flat spots appear shiny because the relatively smooth surface easily reflects light. The finely textured central area contains many small elongated crevices which are the result of delaminations along the banded regions of the microstructure. Figure 16 shows the fracture faces of two different flash welded joints in Inconel 625. The weld fracture B, which is representative of good welding practice, has a fine uniform texture. As indicated by the arrows, fracture face A contains several flat spots which are surrounded by finely textured material. The shiny smooth strip along the lower edge of weld fracture B is the result of arc gouging and is not related to the fracture. Figure 1, page 11, previously discussed, shows the fracture surfaces from a single Hastelloy X weld. (These are mating fracture faces.) The shiny flat spots on these surfaces are indicated by arrows. Relatively flat but shingled regions separate the majority of the flat spots. This fracture



Figure 15. Fracture faces of two different flash welded joints made in Waspaloy.

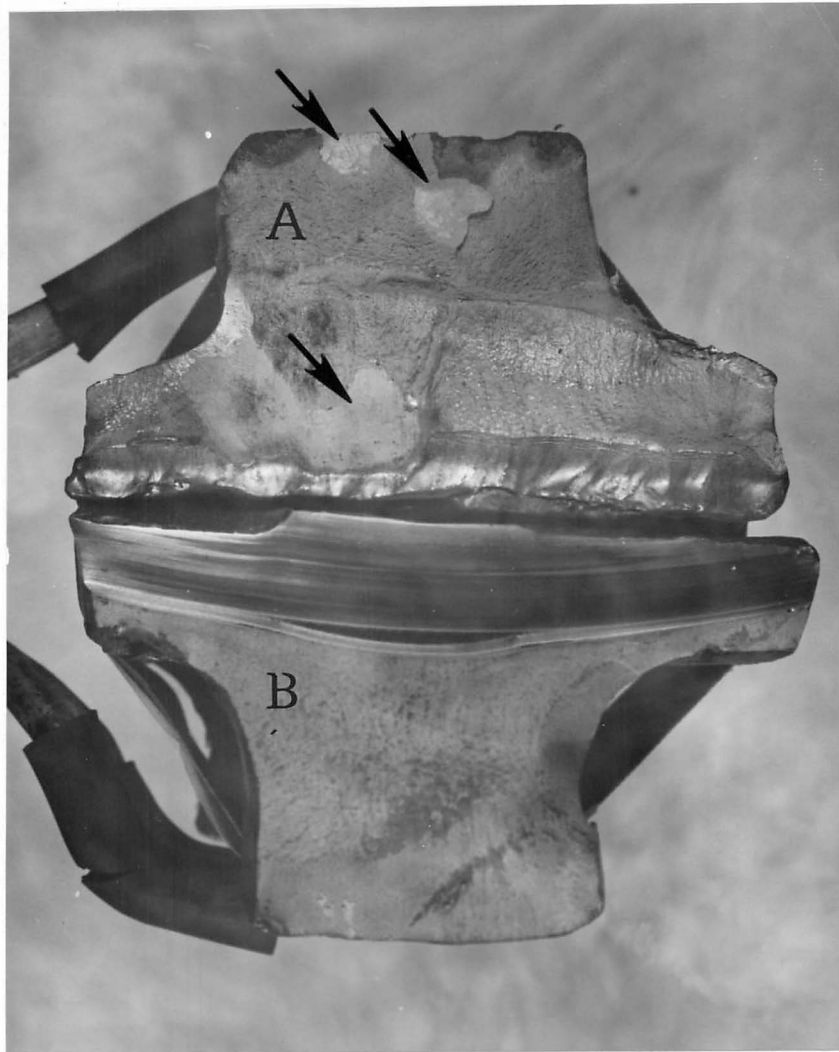


Figure 16. Fracture faces of two different flash welded joints made in Inconel 625.

was confined to the weld interface by notching the specimen with an abrasive cut-off wheel as can be seen on the right and left sides of the fracture. Streaks are also evident on these surfaces.

Figure 17 shows the fracture faces of two different flash welded joints in N-155 material. Again the abrasive cuts which were made to confine the fracture are evident along the sides of the specimen. Fracture surface A exhibits a ductile fracture over the majority of the fracture surface. Some streaking is evident at the left and along the lower edge. In contrast weld B contains only flat spots and streaks. This particular weld was among those exhibiting the lowest ductility of any of the welds investigated. The streaking was very severe occurring over a significant distance across the weld interface as evidenced by differing fracture surface elevations.

Figure 18 shows the fracture faces of two different welded joints in Inconel 718. Weld fracture B shows some streaks along the upper and lower edges. The remaining portion is of a ductile nature. The fracture surface of weld A is essentially one large, pockmarked flat spot and is a fracture indicating extremely low ductility. The pockmarks are flat spots differing in fracture surface elevation.

#### Microscopic Examination of Weld Defects

Macroscopic examination of the weld fracture surfaces revealed the presence of many streaks and flat spots. To better understand these

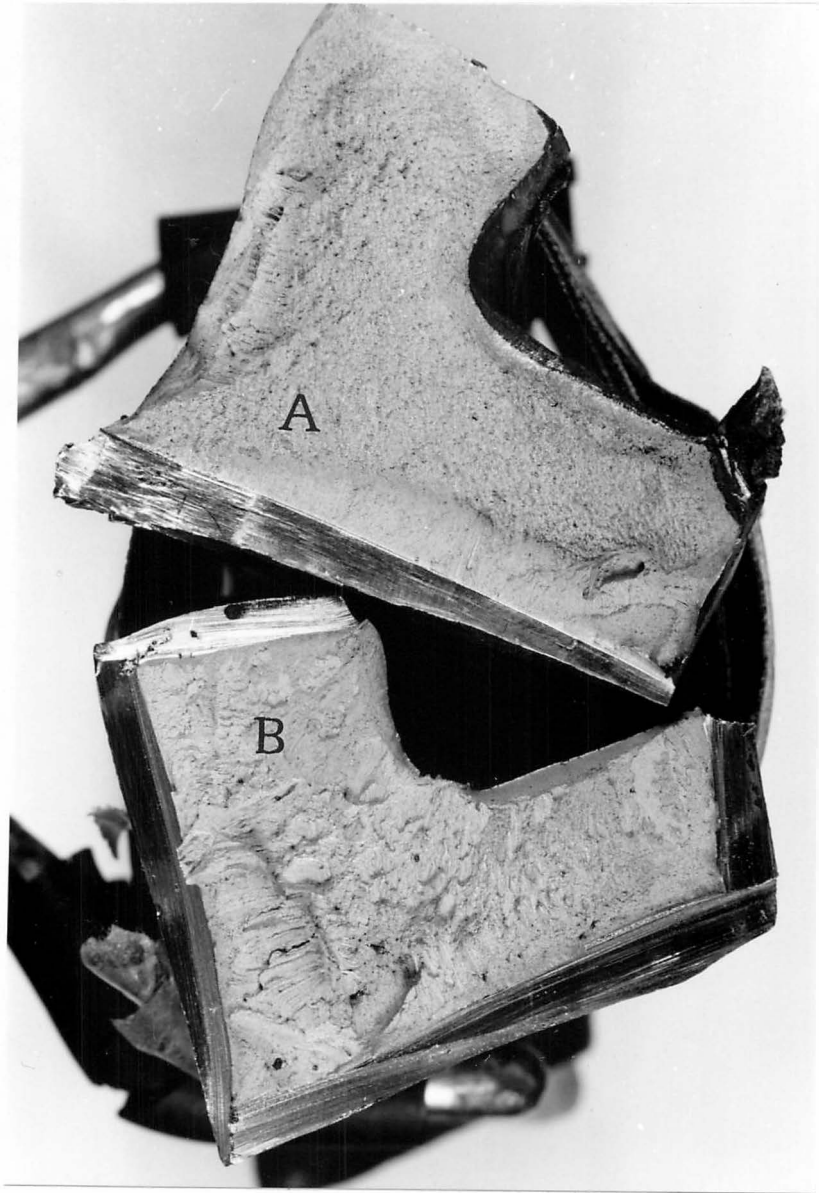


Figure 17. Fracture faces of two different flash welded joints made in N-155.

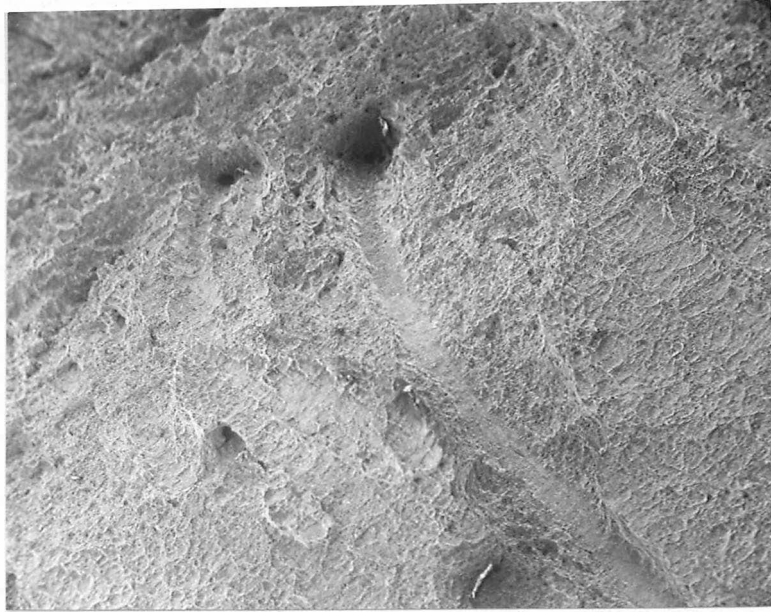




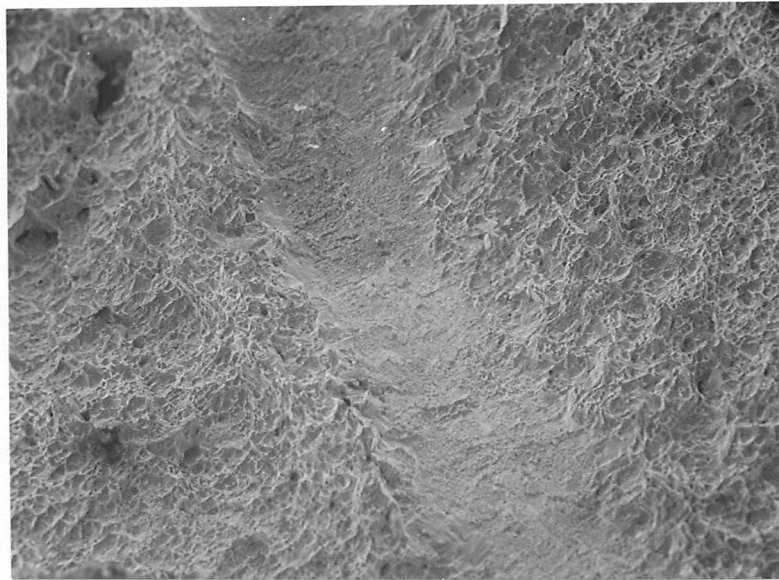
Figure 18. Fracture faces of two different flash welded joints made in Inconel 718.

features, microscopic examination using the optical and scanning electron microscopes was performed.

Figure 19A, an SEM micrograph at 20X, shows the central region of a fracture face from a weld in Waspaloy. A streak can be seen as one of the features on the fracture surface. The streaked region departs from the plane of the fracture face by literally penetrating the surface. This streak is a manifestation of a microstructural segregate band which was deformed during weld upset and then exposed by fracture during the slow bend screening test. The part of the streak which lies essentially on the fracture surface was originally located at or very near the weld interface. The streak is long and narrow and appears flat and smooth at low magnification when compared to the topography of the surrounding fracture surface. Figure 19B, an SEM micrograph at 100X, shows the streak to be relatively featureless although the surrounding area exhibits dimples characteristic of ductile fracture. However, when the magnification is increased to approximately 500X, features can be resolved in the streaked area. Figure 20, SEM micrographs at 500X, show that the topography of the streak is essentially a series of small dimples while the adjacent surface at the same magnification shows relatively large dimples. The dimple sizes are different by about a factor of 10. Figure 21 shows the streak at approximately 2000X. Many particles can be seen located within the dimples. These particles are the initiation sites for void formation and the resultant dimpled

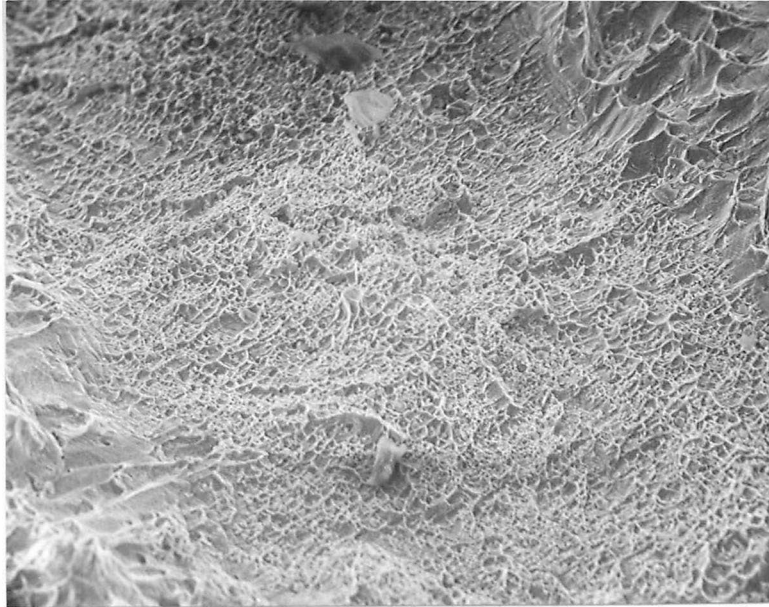


(A) 20X

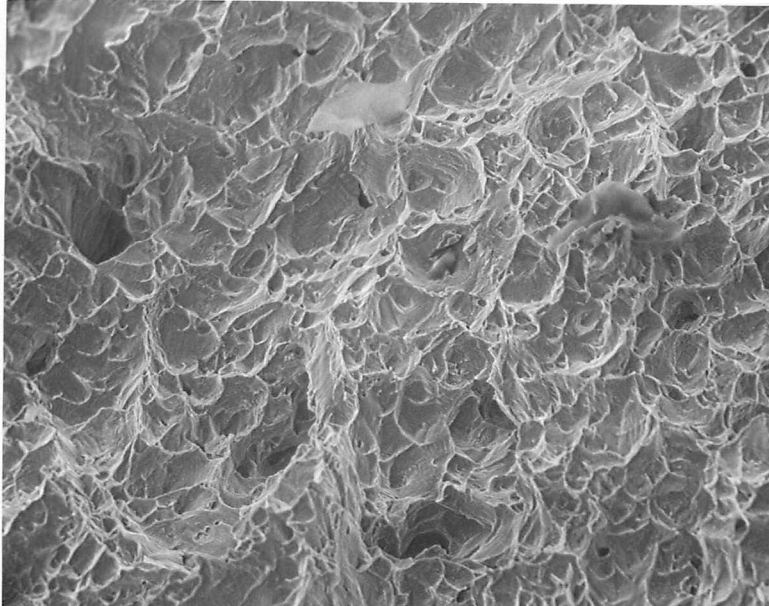


(B) 100X

Figure 19. SEM micrographs of streak on Waspaloy fracture surface.



(A) Streak. 500X



(B) Adjacent surface. 500X

Figure 20. SEM micrographs comparing dimple size on the streak and adjacent area at 500X.

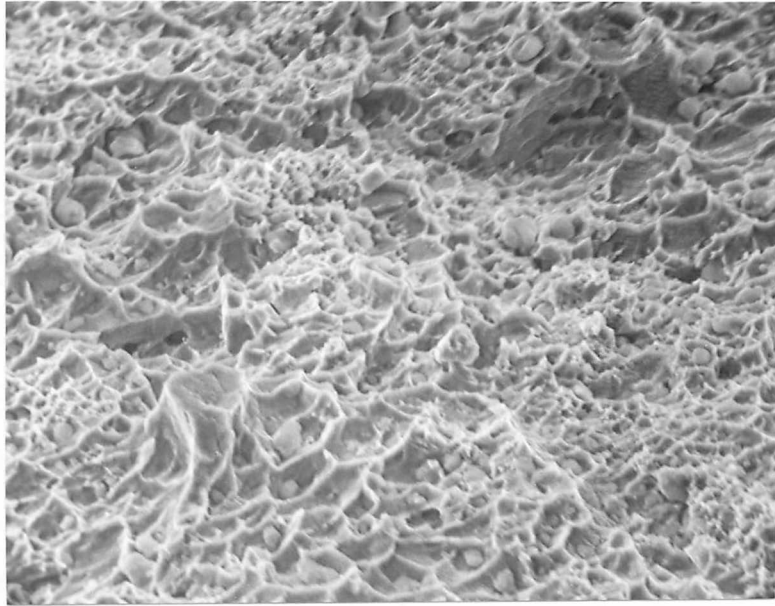


Figure 21. SEM micrograph of streak at 2000X.

structure. As previously mentioned, the difference in dimple size means that the streaked region exhibited less ductility than the surrounding material.

Two parallel streaks were revealed on the fracture face of the Inconel 718 weld specimen shown in the SEM micrograph in Figure 22. Both streaks appear to tunnel into the fracture surface and are bisected by a secondary crack. At 300X (Figure 23A) the streak appears rather flat and smooth when compared to the surrounding surface which exhibits many dimples. When viewed at 3000X (Figure 23B), the streak can be seen to reveal many small dimples. This is another example which shows that streaks exhibit dimples which are much smaller than the material characterized by the surrounding fracture surface topography. This difference of dimple size was evident on all streaks investigated on the weld fracture surfaces in all the alloys studied. Thus, it can be concluded that streaks are the result of fracture along microstructural bands which because of their high particle content fracture in a less ductile manner than the surrounding relatively particle-free material.

Energy dispersive (ED) x-ray analysis was performed on several of the streaks. When streaks in two different Waspaloy fracture specimens were analyzed, the data indicated that the streaked regions contained a much higher concentration of aluminum and a slightly higher concentration of titanium than did the adjacent area. One of the streaks which was analyzed appears in Figure 19, page 54, and was previously discussed. X-ray

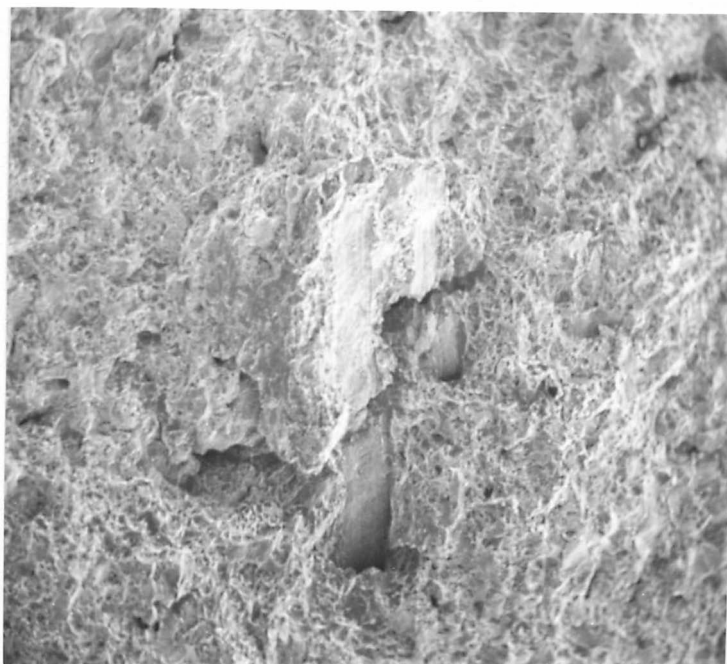
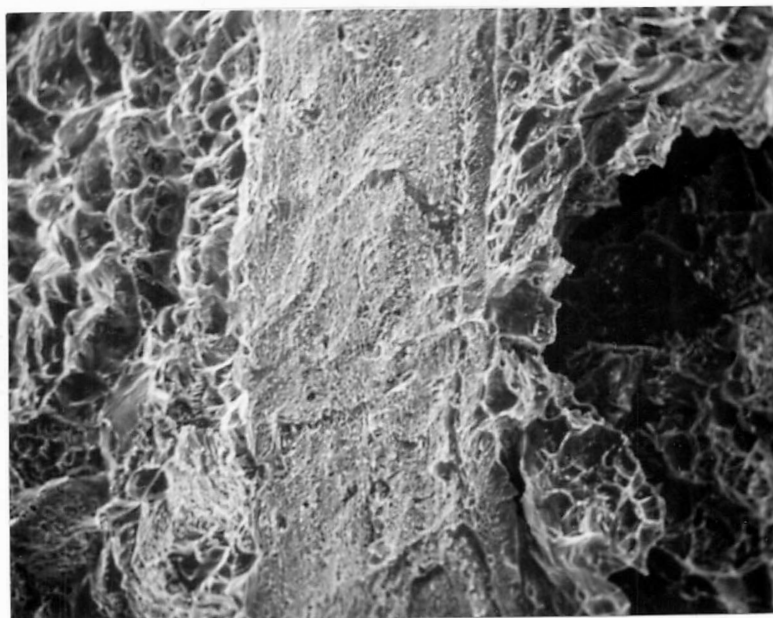
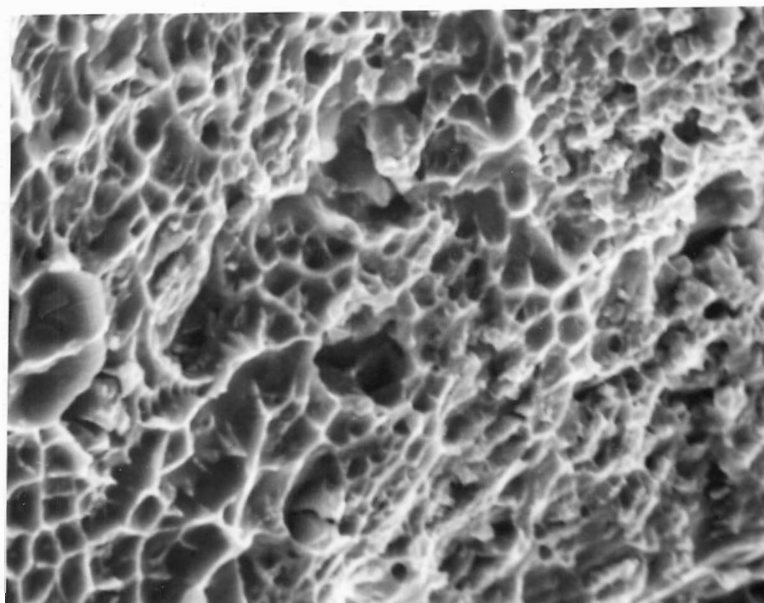


Figure 22. SEM micrograph of streaks on the fracture face of an Inconel 718 weld sample. 70X



(A) 300X



(B) 3000X

Figure 23. Higher magnification SEM micrographs of one streak shown in Figure 22 .



analysis of streaks on several different Inconel 718 fracture specimens showed a similar variation in chemical concentration for aluminum and titanium. However, the titanium concentration variation in these specimens was more pronounced than that revealed for the Waspaloy specimens.

The indicated variation in chemical composition which was mentioned above is qualitative at best. Data of a quantitative nature are difficult to obtain by ED methods on rough fracture surfaces because of several limitations which are:

1. Secondary fluorescence.
2. Varying take-off angle.
3. Limited spectrum sensitivity.

The first difficulty arises because x-rays originating from the analyzed feature may be absorbed by the surrounding matrix while secondary x-rays are created and subsequently analyzed by the detector<sup>(40, 41)</sup>. Thus, the analysis is misleading. Another difficulty of analyzing rough surfaces is that the take-off angle varies as a function of position on the surface. If the specimens were relatively flat or polished, their analysis could be compared to known standards and with the use of corrective equations could yield true quantitative results<sup>(40)</sup>. If particles on the fracture face are to be analyzed, more accurate results are possible by using an extractive replica to remove the particles from the fracture face. This replica is then analyzed using ED techniques. The most accurate analysis of a rough surface by ED spectrography is achieved by optimizing the specimen tilt

angle and increasing the working distance. At best, these results will be semi-quantitative.

Several equipment limitations prevented full spectrum and true quantitative x-ray analysis of the samples studied in this investigation. Full spectrum analysis is impossible because the beryllium window which protects the detector absorbs most of the x-rays produced by elements whose atomic weights are less than sodium. Thus, this equipment is not capable of determining whether the particles contain carbon or oxygen. In addition, the ED system used in this study did not contain a minicomputer for performing the numerous and tedious corrections necessary for true quantitative analysis.

Particle/segregate bands may take on a broad flat character rather than a thin pencillike configuration. The pencillike configuration results in streaks such as those just described above where the length to width ratio is large. As the particle/segregate bands become wider relative to their length, the streaks take on a more equiaxed shape intermediate between "streaks" and "flat spots". A region of this sort is shown in the SEM micrographs of Inconel 718 in Figure 24. The parallel, flat rectangular areas which are separated by rougher, more ductile regions resemble streaks although they are wider than most. They are also similar to flat spots since they form regions which are separated from the surrounding more ductile areas by differences of elevation and fracture appearance. Flat spots are invariably characterized by abrupt elevation changes from

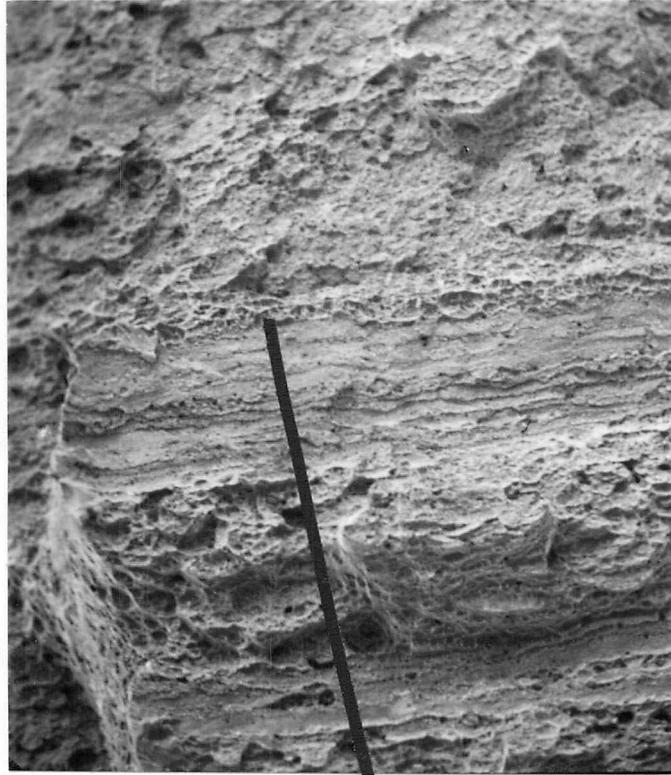
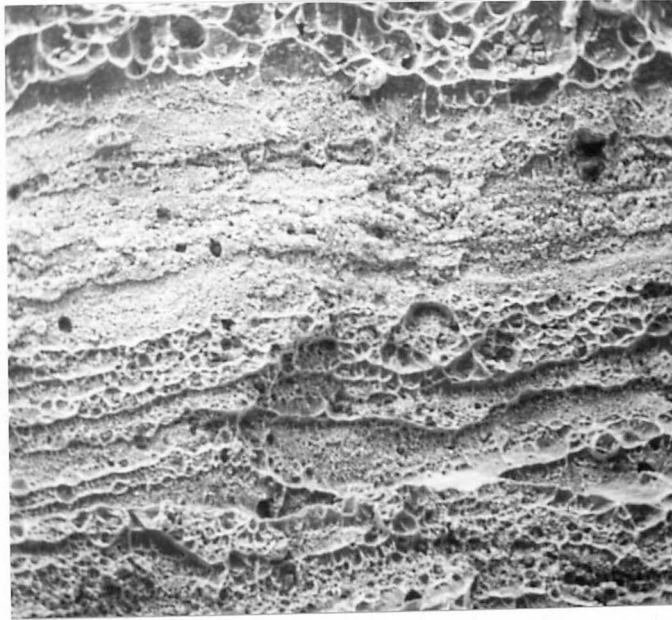


Figure 24. SEM micrograph of a fractured intermediate width particle/segregate band. 100X

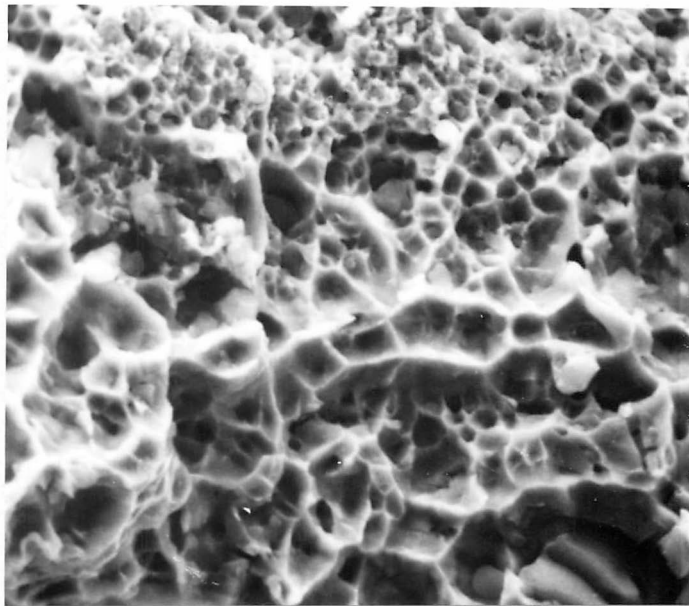
the surrounding more ductile regions. Figure 25, SEM micrographs, shows this feature at higher magnifications. Many dimples of varying sizes are visible. Like streaks, these areas fractured by the formation and coalescence of microvoids. The bands of particles which nucleated fractures in these areas were much wider than those resulting in streaks.

The structure shown in Figure 24 was sectioned perpendicular to the fracture surface to reveal the bulk microstructural features adjacent to the fracture surface. The sectioning line is also shown in Figure 24. Figure 26 shows the microstructure at two locations along the sectioning line. These light micrographs at 750X magnification show typical particle distributions. The arrows indicate particles appearing on the fracture surface. The fracture surfaces were nickel-plated to help retain the surface particles. It should be noted that the particles are not randomly distributed but probably reflect prior particle segregate morphology as modified by the thermal and mechanical history during welding.

"True flat spots" characterized by broad, equiaxed, low ductility regions differing in elevation from surrounding fracture surface features appear to be the result of two primary mechanisms. One mechanism consists of fracture along broad flattened particle/segregate regions in much the same manner as that described for streaks. The other mechanism revealed by this study is one in which faying surface oxidation plays an important role.

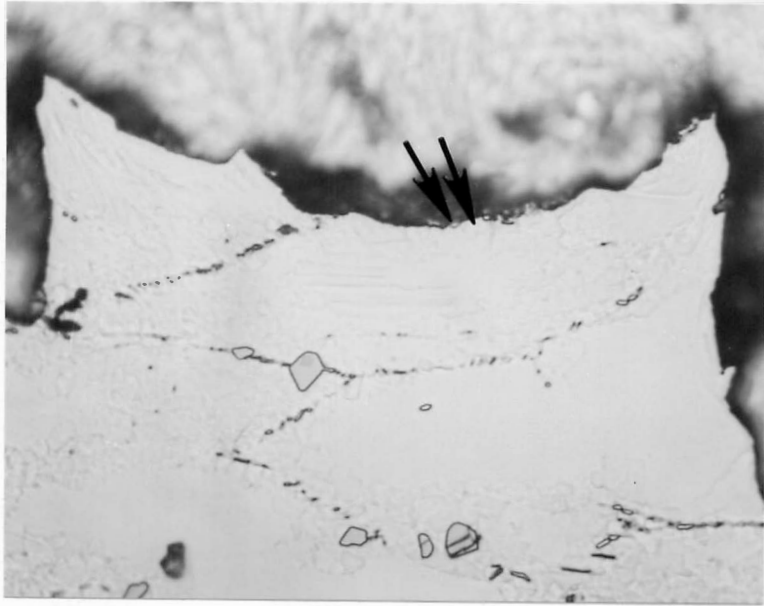


(A) 300X

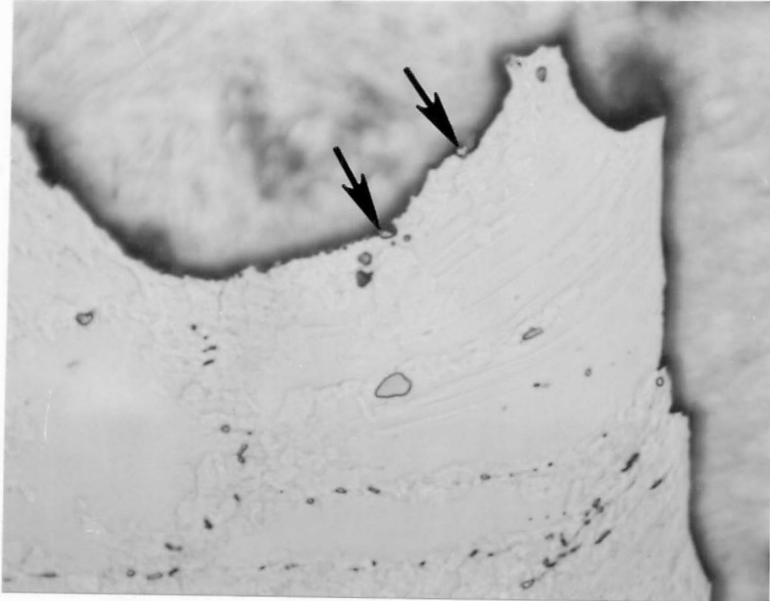


(B) 3000X

Figure 25. Higher magnification SEM micrographs of feature shown in Figure 24.



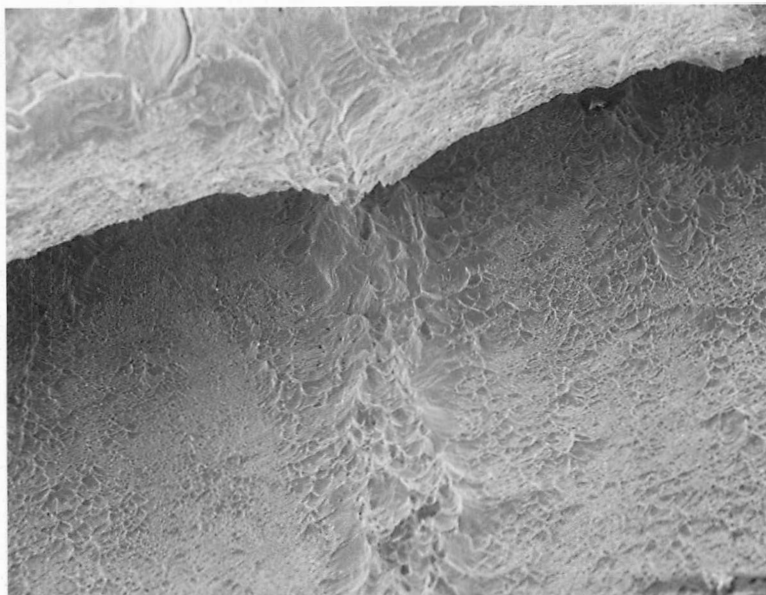
(A) 750X



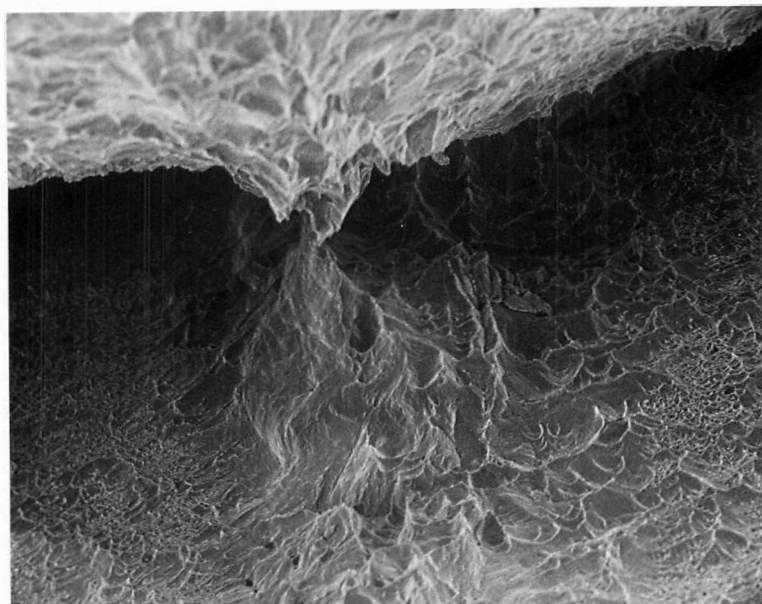
(B) 750X

Figure 26. Microstructure at two locations along the sectioning line shown in Figure 24.

If broad flat microstructural particle/segregate bands are oriented such that they are essentially parallel to the weld interface and thus perpendicular to the principal stress applied during bend testing, a large low ductility region will generally result from fracture propagation through these regions. A flat spot which formed by this process is shown in the SEM micrographs in Figure 27. The previously propagating but now arrested crack is shown. One should visualize that the fracture surfaces are created by crack propagation which separates one strata from another in much the same manner as peeling tape from a flat surface or removing the outer covering from a banana. When viewing Figure 27A, one should visualize that the material in the upper half of the micrograph is being peeled away from the lower flat portion thus creating two surfaces. The true leading edge of the fracture is seen at only one point along the crack front shown in Figure 27. This point is at the center of the micrograph and is characterized by the rough large dimpled region. The leading edge at the other locations is under the upper peeled portion. The crack front is thus scalloped while propagating. This is a result of the local variation in ductility as a smaller strain is required to separate low ductility regions than the high ductility regions. The broad flat areas exhibit low ductility because of the high particle density. Figure 27B shows that the overhang is still attached to the lower surface in the rougher areas. The two surfaces have already completely separated in the surrounding flat region. Figure 28 compares the dimple size in the rougher strip (Figure



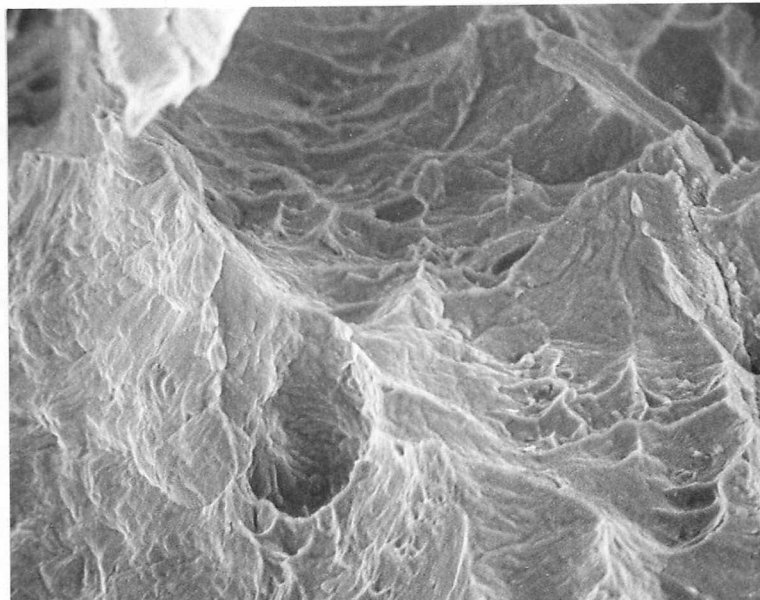
(A) 160X



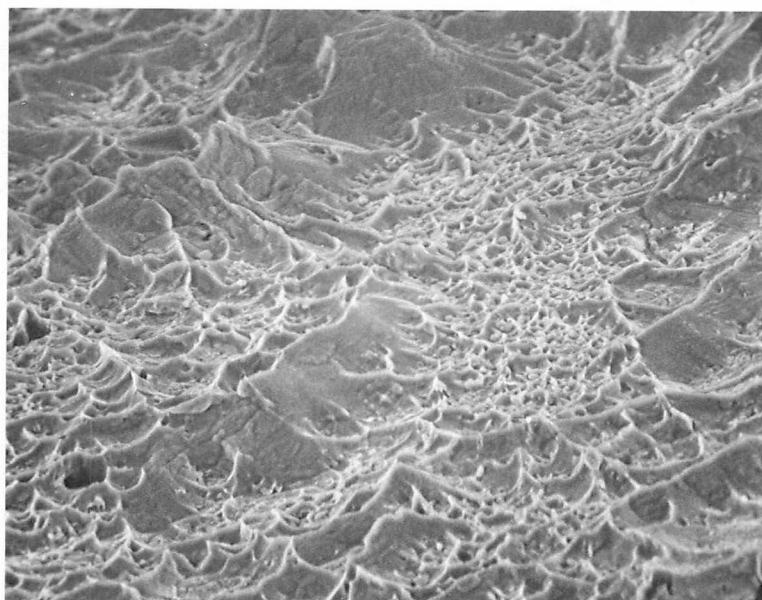
(B) 375X

Figure 27. Flat spot caused by broad, flat microstructural particle bands.





(A) Rough area. 1500X



(B) Flat spot. 1500X

Figure 28. SEM micrographs comparing the dimple size on the rough and flat areas of Figure 27.

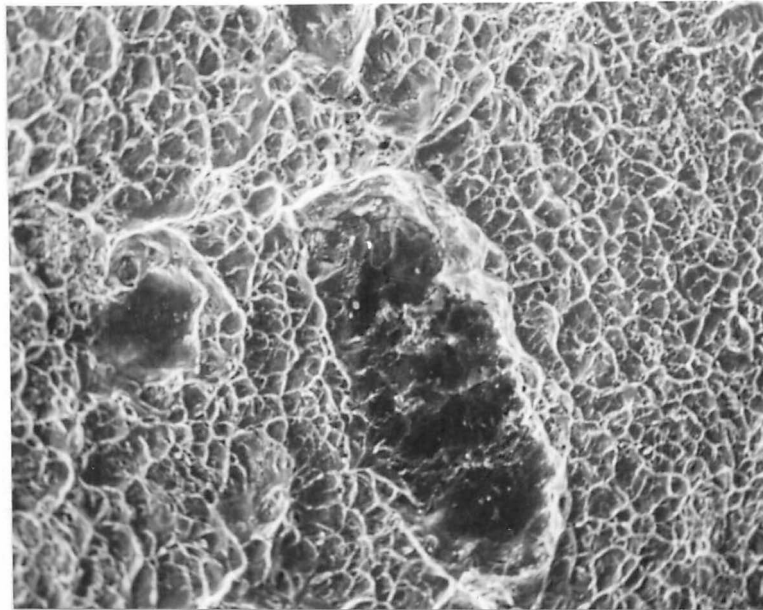
28A) with the size on the surrounding flat region (Figure 28B). These micrographs show vividly that the larger dimpled fracture surfaces have undergone greater plastic strain than the smaller dimpled areas.

The other mechanism responsible for flat spots is the entrapment of oxide pools or films at the weld interface. Figure 29A, SEM micrograph at 100X, shows several dark areas which appear on the fracture face of an Inconel 625 weld sample. These areas are surrounded by a dimpled fracture surface. Figure 29B shows one of the dark areas at higher magnification. Figure 30A shows the dark area at still higher magnification (3000X) where the dark area appears rather flat and is cracked similar to a dried-up mud puddle. A larger but similar dark area from the same sample was sectioned by cutting perpendicular to the fracture face. A micrograph representative of the polished specimen at the fracture edge appears as shown in Figure 30B. The dark color and shape of the surface constituent indicates that it is an oxide. ED spectroscopy indicated that titanium and aluminum were major constituents of the oxide area while, in contrast, adjacent areas of the fracture face contained only minor concentrations of these elements. Since these two elements are probably the most easily oxidized of all the elements contained in this alloy, this composition difference would be anticipated if oxidation of the faying surface had occurred during flash welding.

Figure 31, an SEM micrograph at 100X magnification, shows a flat spot on the fracture face of a Hastelloy X flash weld. At this low

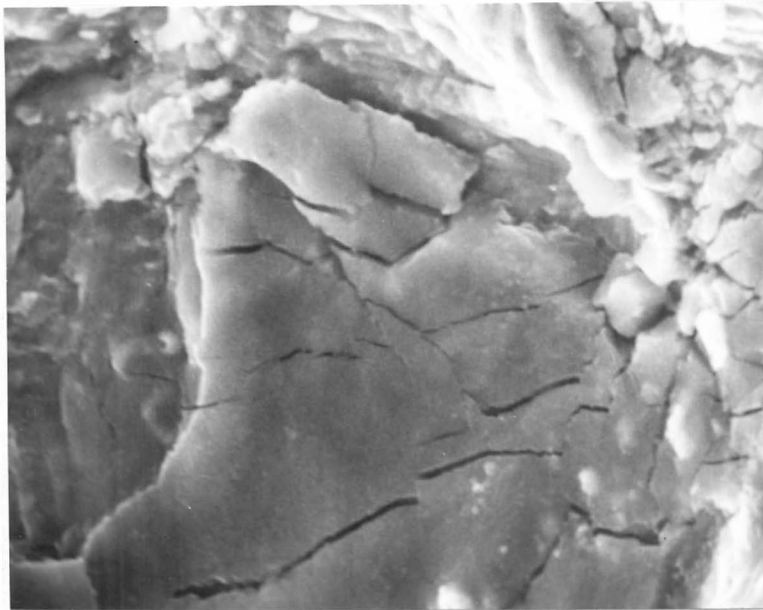


(A) 100X

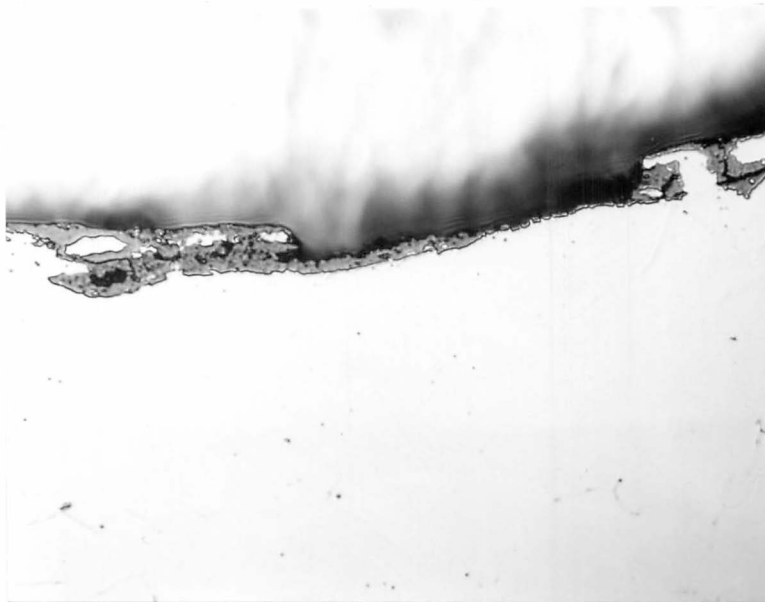


(B) 300X

Figure 29. SEM micrographs showing dark areas on the fracture face of an Inconel 625 weld sample.



(A) SEM micrograph. 3000X



(B) Light micrograph. 500X

Figure 30. High magnification SEM and light micrographs of the dark area shown in Figure 29.

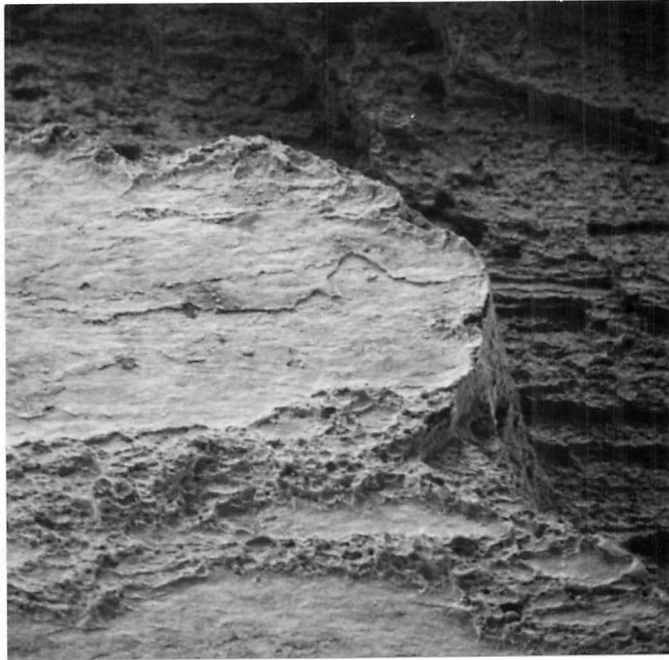


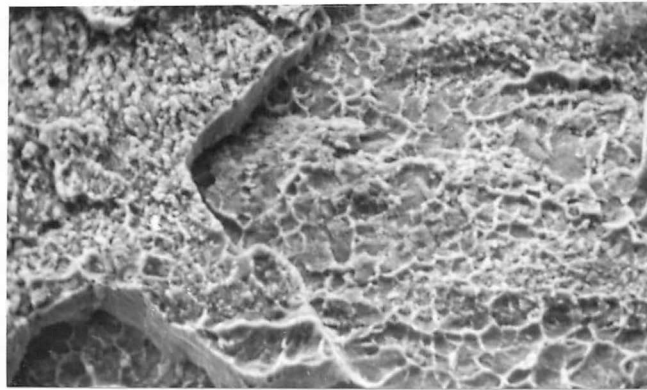
Figure 31. Flat spot on fracture face of a Hastelloy X flash weld.  
100X

magnification, the flat spot resembles a mesa which is divided by a rougher region. Figure 32, SEM micrographs, shows this flat spot at successively higher magnifications. At 3000X (Figure 32C) the flat spot exhibits some dimples which appear to be partially filled by a scaly oxide. Although this brittle appearing oxide is not continuous over the affected area, its presence is deleterious enough to reduce the ductility of the welded joint. This specimen was sectioned perpendicular to the fracture face and through the flat spot. After polishing and etching, optical micrographs were obtained from the region at the fracture interface. Figure 33A and B, light micrographs at 500X and 750X, respectively, shows typical areas along the interface of the flat spot. (Note the sunburst effect which appears in the upper half of each micrograph. This is the nickel plating which was added for improved edge retention during polishing.) Oxide films can be seen along the interface and just below the surface of the flat spots. X-ray analysis indicated that aluminum was present in this oxide film, but it was not detected in the rougher, more ductile area which divided the flat spot into two distinct regions. Aluminum is not an intentional alloying element in this alloy, but it is often present in the scrap material which is added to complete a furnace charge.

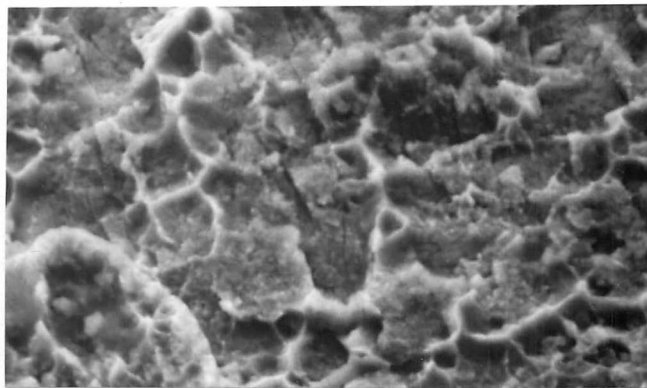
Occasionally a flat spot indicates the presence of both an oxide film and an area exhibiting high particle density. Figure 34, SEM micrographs at 15X and 170X, illustrates such an occurrence. The peeled-up area is an oxide film which constitutes a portion of the flat spot. The



(A) 300X

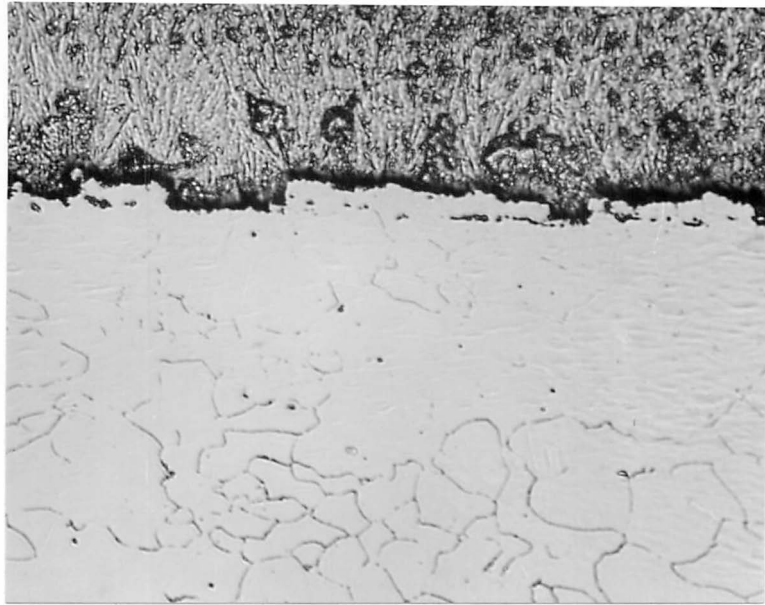


(B) 1000X

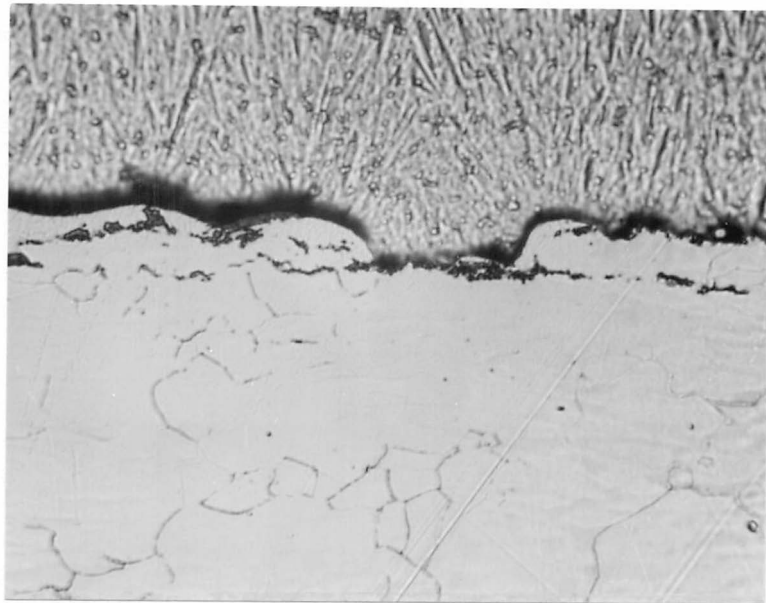


(C) 3000X

Figure 32. Flat spot shown in Figure 31 at higher magnifications.



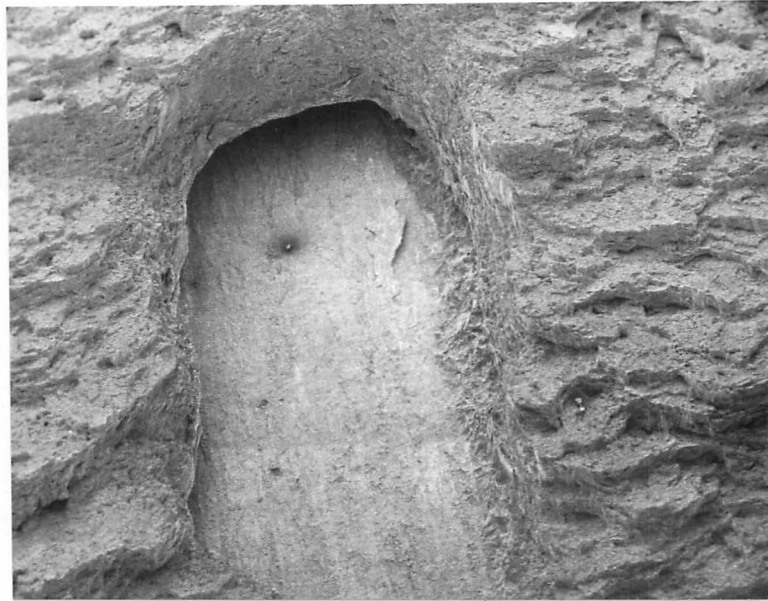
(A) 500X



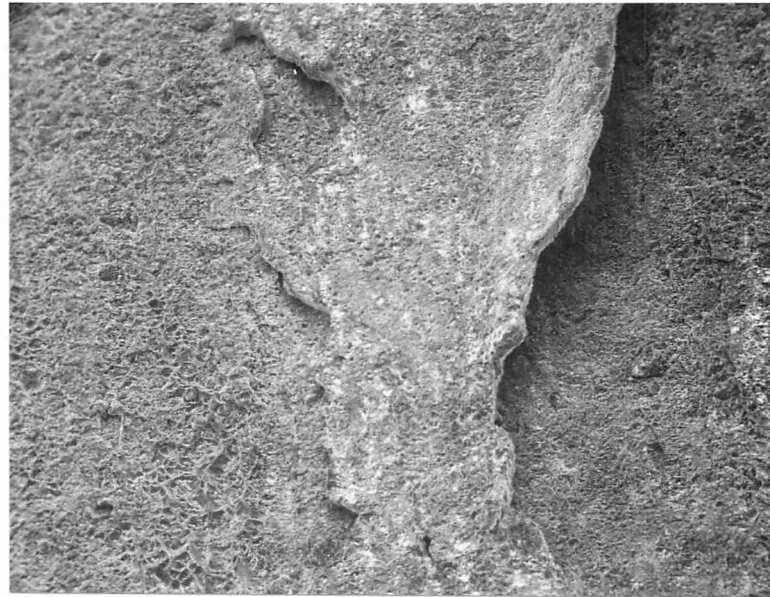
(B) 750X

Figure 33. Light micrographs showing typical areas along the interface of the flat spot shown in Figure 31.





(A) 15X



(B) 150X

Figure 34. SEM micrographs of pockmarked oxide film on a flat spot.

oxide film is pockmarked by numerous particles. Figure 34A, page 76, also shows the shingled feature which was previously discussed but not illustrated. The shingled region exists to either side of the flat spot. The shingles are caused by the interconnection of parallel particle/segregate bands which have been fractured for only short distances and then sheared across more ductile regions to another similarly oriented particle/segregate band. These features are often found on flash weld fracture surfaces and while not considered "flat spots" are never-the-less regions of low ductility.

The data which this investigation has yielded show that the base material microstructure is often as important as the process variables in influencing the ductility of a flash welded joint. For a given set of process parameters, the ductility of a welded joint may have a significant dependence upon the microstructure of the base material. The results of this investigation also imply that the process variables may be altered to minimize the deleterious effects of the base metal microstructure.

For example, a clean and lightly banded base metal may be upset significantly during welding so that the microstructural bands are turned outward, and yet, a continuous or semi-continuous network of low ductility fracture paths does not exist. In fact, upset of a significant degree may be an advantage in eliminating crater related oxide films. However, a heavy upset in a deleteriously banded base material may result in continuous low ductility fracture paths at the interface and this alone would

produce an unacceptable weld. In this case, a minimum upset would be in order even though the formation of crater related oxidized films would be enhanced.

There may be cases in which the base material is so adversely banded that it would not be possible to produce a weld of suitable ductility. If sufficient documentation were available for a given base material, it would be possible to establish weldability acceptance criteria based on the microstructure of the as-received materials.

Many specimens were examined in which the base material microstructure adversely affected the ductility of the welded joints. The defects used for illustration in the foregone discussion are only a few of the many similar appearing features which were uncovered and studied in this investigation.

The streaks shown in Figures 19 through 21, pages 54 through 56, respectively, and Figures 22 and 23, pages 58 and 59, respectively, were caused by the particle/segregate bands which were preferential paths for fracture propagation. The numerous particles nucleate microvoids which propagate for only short distances before intersecting neighboring microvoids to form adjacent dimples on the fracture faces. Thus, the particle bands became streaks or flat spots whose dimples are much smaller than those on the adjacent surface. These particle/segregate bands fractured easily because the high particle densities reduced the total strain to failure and thus the ductility. The flat spot shown in Figures 27 and 28,

pages 67 and 68 , respectively , resulted from a flattened particle/segregate band or bands . In contrast, the flat spots shown in Figures 29 and 30 , pages 70 and 71 , respectively , and Figures 31 through 33 , pages 72, 74 , and 75 , respectively , were caused by incorrect process variables such as insufficient upset , non-parabolic platen movement , and/or excessive voltage which resulted in entrapment of brittle oxides . These oxides were found by ED spectrography to be enriched in aluminum and titanium .

Other material-related phenomena may affect the ductility of flash welded joints . The imposed thermal cycle may cause dissolution of second-phase particles . The dissolution of these particles should raise the yield strength near the weld interface because of an enhanced solid solution strengthening effect . Reprecipitation of these particles is also possible , and the most probable sites are along grain boundaries . A network of grain boundary precipitates could be detrimental because it forms a fracture path which requires little strain to failure by nucleation and coalescence of microvoids . In addition, the thermal cycling may cause constitutional liquation of some particles which can both enrich the surrounding matrix and possibly wet grain boundaries resulting in intergranular failure during subsequent fabrication operations or in actual service .

Other investigators<sup>(18)</sup> have proposed that flat spots are caused by entrapped liquid metal pools of modified composition which solidify to become brittle regions at the weld interface . No indication of entrapped

liquid metal pools was found in any samples from this investigation. However, it must be recognized that the upset of the material during the flash welding cycle may completely obscure this phenomenon. Recrystallization can and does take place during cooling at the weld interface after upset, and this too tends to obliterate some high temperature microstructural phenomena.

To reiterate, this investigation showed that when flat spots appear on a flash weld fracture surface they usually exhibit upset, flattened, and solidified oxide pools. The remaining fracture surface will exhibit dimples.

## CHAPTER IV

### CONCLUSIONS

The fracture morphology studies conducted on flash welds in five iron-nickel base superalloys yielded the following conclusions:

1. The base materials used in this study exhibited banded microstructures in which the particle/segregate bands were elongated primarily parallel to the longitudinal axis. The orientation between these banded microstructural features and a propagating crack influence the fracture path. This, in turn, determines the fracture surface appearance and weld ductility.
2. The complex geometrical base material configurations used in this study yield complicated upset deformation patterns during flash welding. Thus, many different and changing orientations are encountered by a propagating crack as it traverses the banded microstructure throughout the cross section of a slow bend test specimen. Therefore, the fracture face appearance will vary from location to location.
3. On every fracture surface studied a dimpled appearance predominated. Thus, the fractures progressed primarily by the initiation and coalescence of microvoids. However, the mere

presence of dimples on a microscale does not necessarily indicate macroscopic ductility. One exception to the microvoid mechanism is fracture propagation through an entrapped oxide film which formed during flashing. A flat spot is created where fracture occurs by this means. Oxides of aluminum and titanium are the primary constituents of the defect which has this morphology. All other flat spots and streaks are caused by bands of high particle density which become preferential paths for fracture propagation. The total strain to fracture is very low in these regions even though fracture occurs by the initiation and coalescence of microvoids. Thus flat spots and streaks appear flat at low magnification but many exhibit dimples at high magnification. These dimples are considerably smaller than those on the adjacent low particle density fracture surface.

4. Dissolution of second-phase particles occurs as the weld interface is approached. The dissolution of particles should raise the yield strength near the weld interface because the matrix will be solid solution strengthened. Reprecipitation of particles is also possible, and the most probable sites are along grain boundaries. Grain boundary precipitates in large numbers can be detrimental because they present a fracture path which requires little strain for the initiation and

coalescence of microvoids , and thus the ductility of the welded joint is reduced .

5. Constitutional liquation was observed in several samples .  
The presence of cracks in several of the constitutionally liquated regions indicate that these areas are subject to failure at low strains . These areas are not necessarily at the faying interface but may be a significant distance away and , therefore , may not be detected in the destructive slow bend test used for screening .



## CHAPTER V

### FUTURE WORK

The specimens studied in this investigation were selected for their fracture surface appearance and for being representative of the types and magnitude of defects encountered during the development of a flash welding schedule. While they are typical, their selection was not based on statistical sampling techniques.

In future studies, specimens for examination should be selected by a true statistical sampling method. The nature and frequency of occurrence of flash weld defects should be documented as a function of flash weld parameters. Using the optimum flash weld parameters, an even larger statistically valid sample should be selected and tested to determine the probability of occurrence of a major defect. In studies of this sort, a simple square cross sectioned bar should be chosen and the same heat of material used throughout. The investigation should also include the effect of notch orientation relative to the weld interface on fracture appearance.

A second investigation which should be undertaken involves the more complete determination of the formation of oxide and particle/segregate banded flat spots. In this study a set of optimum weld parameters

should be selected for a simple square bar and samples prepared with the upset varied from zero to an amount in excess of the optimum. This would enable the mode of crater collapse and oxide entrapment to be followed and also the degree and influence of banding turn-out to be documented. Again a statistical number of samples should be chosen for each upset.

A third investigation would be to document the properties and fracture mode of the base material when tested in the short transverse direction. This study should yield information which will help to define the as-received material-related parameters on weld defect occurrence.

It is suggested that all three of the above investigations be carried out simultaneously using the same heat of base material. An investigation of this sort should provide statistical information upon which the probability of defect occurrence could be predicted and thus could be helpful when used as a manufacturing quality control technique.

LIST OF REFERENCES

## LIST OF REFERENCES

1. Savage, W. F., "Flash Welding - The Process and Applications," Welding Journal, 41 (3), pp. 227-237, 1962.
2. "Flash and Friction Welding," Welding and Brazing, Metals Handbook, Vol. 6, pp. 485-518, American Society for Metals, Metals Park, Ohio, 1971.
3. Savage, W. F., "Flash Welding - Process Variables and Weld Properties," Welding Journal, 41 (3), Research Supplement 190-s to 119s, 1962.
4. Nippes, E. F., Savage, W. F., Grotke, G. and Robelotto, S. M., "Further Studies of the Flash Welding of Steels," Welding Journal, 34 (5), Research Supplement 223-s to 240's, 1955.
5. Riley, J. J., "Flash-Butt Welding - Welding Technique and Variables in Welding Low-Alloy Steels," Welding Journal, 24 (1), Research Supplement 12-s to 24-s, 1945.
6. Williams, N. T., "Influence of Welding Cycles on the Ferrite Content of Type 321 Austenitic Steel," British Welding Journal, 12 (9), pp. 435-441, 1965.
7. Summerfield, A. J. and Apps, R. L., "A Metallographic Study of the Incidence of Cracking in Stainless Steel Flash Welds," Metal Construction and British Welding Journal, 1 (2s), pp. 86-92, 1969.
8. Forostovels, B. A. and Dem'Yanchuk, A. S., "Chemical Heterogeneity in Flash Welds in Heavy Section Steel," Automatic Welding, 20 (6), pp. 30-34, 1967.
9. Forostovels, B. A., "Conditions Under Which a Bright Band Forms in Flash Welded Joints Made with Continuous Flashing," Automatic Welding, 21 (9), pp. 18-23, 1968.

10. Johnson, K. I., "An Approach to Quality Control of Some Flash Welded Components," Proceedings of Advances in Welding Processes, pp. 99-105, The Welding Institute, Cambridge, 1971.
11. Faulkner, F. J. S. and Shaw, J., "Flash Welding of Rails for London Transport," Proceedings of Advances in Welding Processes, pp. 34-39, The Welding Institute, Cambridge, 1971.
12. Yavorskii, Y. D., "Effects of the Welding Conditions on the Surface Profile During Flash Welding," Automatic Welding, 17 (11), pp. 15-19, 1964.
13. Kilger, H., "Production Technique and Quality of Flash Welded Joints," (translation), Welding Journal, 24 (9), Research Supplement 459-s to 480-s, 1945.
14. Hess, W. F. and Muller, A., "The Flash Welding of Nickel and High-Nickel Alloy Rod," Welding Journal, 22 (10), pp. 532-544, 1943.
15. Barrett, J. C., "Flash Welding of Alloy Steels Physical and Metallurgical Characteristics," Welding Journal, 24 (1), Research Supplement 25-s to 44-s, 1945.
16. Nippes, E. F., Savage, W. F., Grotke, G. and Robelotto, S. M., "Studies of Upset Variables in the Flash Welding of Steels," Welding Journal, 36 (4), Research Supplement 192-s to 216-s, 1957.
17. Gordon, P. H. and Young, W. F., "Flash Butt Welding of Heavy Sections," British Welding Journal, 14 (12), pp. 619-626, 1967.
18. Sullivan, J. F. and Savage, W. F., "Effect of Phase Control on Flash Weld Defects," Welding Journal, 50 (5), Research Supplement 213-s to 221-s, 1971.
19. Simmons, W. F. and Gunia, R. B., Compilation of Trade Names, Specifications, and Producers of Stainless Alloys and Superalloys, American Society of Testing Materials, Philadelphia, 1969.

20. "Microstructure of Wrought Heat-Resisting Alloys," Atlas of Microstructures, Metals Handbook, Vol. 7, pp. 157-176, American Society for Metals, Metals Park, Ohio, 1972.
21. Everhart, J. L., Engineering Properties of Nickel and Nickel Alloys, pp. 37-81, Plenum Press, New York, 1971.
22. "Databook," Metal Progress, Vol. 104, p. 119, 1973.
23. "Inconel 625," Technical Bulletin T-42, International Nickel Company, New York, 1968.
24. "Inconel 718," Technical Bulletin T-39, International Nickel Company, New York, 1968.
25. Hall, A. M. and Beuhning, V. F., Thermal and Mechanical Treatments for Nickel and Some Nickel-Base Alloys: Effects on Mechanical Properties, NASA SP-5106, United States Printing Office, Washington, D. C., 1972.
26. Johari, O., "Comparison of Transmission Electron Microscopy and Scanning Electron Microscopy of Fracture Surfaces," Journal of Metals, 20 (6), pp. 26-32, 1968.
27. Brandon, D. G., Modern Techniques in Metallography, Butterworths, London, 1966.
28. Bunshah, R. F. (ed.), "Electronic Imaging Techniques," Techniques of Metals Research, Vol. II, Interscience Publishers, New York, pp. 89-91, 1968.
29. Sandberg, A. O., "Energy Dispersion X-Ray Analysis with Electron and Isotope Excitation," Energy Dispersion X-Ray Analysis: X-Ray and Electron Probe Analysis, pp. 113-124, American Society of Testing Materials, Philadelphia, 1971.
30. Walter, F. J., "Characterization of Semiconductor X-Ray Energy Spectrometers," Energy Dispersion X-Ray Analysis: X-Ray and Electron Probe Analysis, pp. 82-112, American Society of Testing Materials, Philadelphia, 1971.

31. Russ, J. C., "Energy Dispersion X-Ray Analysis on the Scanning Electron Microscope," Energy Dispersion X-Ray Analysis: X-Ray and Electron Probe Analysis, pp. 154-179, American Society of Testing Materials, Philadelphia, 1971.
32. Myklebust, R. L. and Heinrich, K. F. J., "Rapid Quantitative Electron Probe Microanalysis with a Nondiffractive Detector System," Energy Dispersion X-Ray Analysis: X-Ray and Electron Probe Analysis, pp. 232-242, American Society of Testing Materials, Philadelphia, 1971.
33. Jubb, J. E. M., "Lamellar Tearing," WRC Bulletin 168, Welding Research Council, Miami, 1971.
34. Oates, R. P. and Stout, R. D., "A Quantitative Weldability Test for Susceptibility to Lamellar Tearing," Welding Journal, 52 (11), Research Supplement 481-s to 491-s, 1973.
35. Pelloux, R. M., "Fractography - The Analysis of Fracture Surfaces by Electron Microscopy," Failure Analysis, pp. 23-42, American Society for Metals, Metals Park, Ohio, 1969.
36. Reed-Hill, Robert E., "Fracture," Physical Metallurgy Principles, pp. 519-570, Van Nostrand Company, Princeton, New Jersey, 1968.
37. Passoja, D. E., "A Dislocation Model for Impact Energy in Metals," TTC-27, Union Carbide Corporation, Tarrytown, New York, June 1973.
38. Widgery, D. J., "Deoxidation Practice and Toughness of Mild Steel Weld Metal," M/76/73, The Welding Institute, Cambridge, England, June 1973.
39. Pepe, J. J. and Savage, W. F., "Effects of Constitutional Liquation in 18-Ni Managing Steel Weldments," Welding Journal, 46 (9), Research Supplement 411-s to 422-s, 1967.
40. "Modern X-Ray Analysis II," EDAX International, Prairie View, Illinois, 1972.
41. Ferrell, R. E. and Paulson, G. G., "Energy Dispersive Analysis of X-Ray Spectra Generated in the SEM," Materials Evaluation Laboratory Incorporated, Baton Rouge, Louisiana, 1973.

## BIBLIOGRAPHY



## BIBLIOGRAPHY

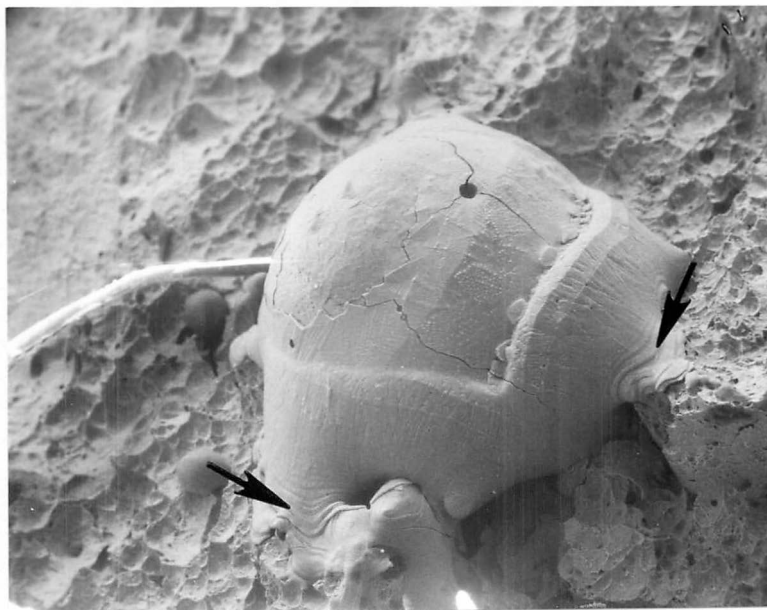
1. Grover, Bennett and Foley, "Fatigue Properties of Flash Welds," Welding Journal, 24 (11), Research Supplement 599-s to 617-s, 1945.
2. Asnis, A. E. and Kuchuk-Yatsenko, S. I., "The Static and Fatigue Strengths of Flash Butt Welding Joints in Large Cross Section Rolled Sections," Automatic Welding, 13 (12), pp. 12-18, 1960.
3. Kuchuk-Yatsenko, S. I., "The Effects of the Final Flashing Stage on the Quality of Flash Butt Welded Joints," Automatic Welding, 15 (7), pp. 31-36, 1962.
4. Agafonov, N. G., et al., "Some Reasons for the Development of Defects During the Flash Welding of Rails," Automatic Welding, 20 (5), pp. 27-31, 1967.
5. Forostovets, B. A. and Kuchuk-Yatsenko, S. I., "Grade 9Kh Steel Welded by the Continuous Flashing Process," Automatic Welding, 21 (5), pp. 25-28, 1968.
6. Sakhatskii, G. P., "Flash Welding with Flux Shielding," Automatic Welding, 25 (1), pp. 42-44, 1972.
7. Thornton, P. R., "Scanning Electron Microscopy - Applications to Materials and Device Science," Chapman and Hall, London, 1968.
8. Langhardt, W., "Improving the Toughness of Flash Butt Welds in Carbon Steels by Pulsation Normalizing and Hot Upsetting in the Welding Machine," Schrveissen and Schneiden, 25 (1), p. 26, 1973. (Brutcher Translation 9043, Altadena, California.)

## APPENDIX

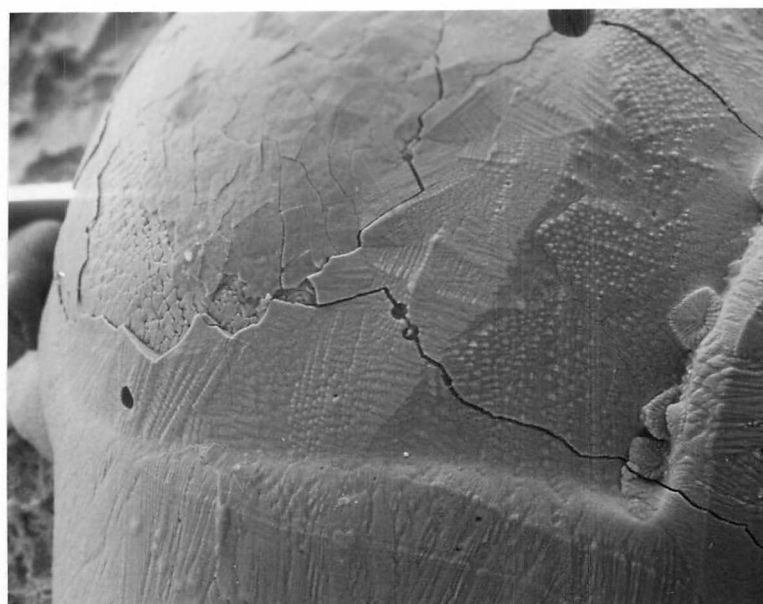
## APPENDIX

During the course of this investigation, many artifacts or otherwise inexplicable features were found on the specimen fracture surfaces. Most of these artifacts were spherical or hemispherical in nature and appeared to have an oxidized surface or skin.

An example of one of these features can be seen in the SEM micrograph in Figure 35A. This feature is roughly hemispherical in shape but has a slight tendency to wet the fracture surface. The thick "collar" around the base of the "blob" in this figure resembles a taffy apple whose candy coating has begun to run from the surface. The arrows indicate ripples which probably formed as the "blob" struck the fracture surface and solidified. Some cracks are visible on the surface of the "blob". A bright fiber can be seen on the fracture surface. Similar bright "charged" fragments are often encountered in SEM microscopy. Figure 35B shows the "blob" at 500X magnification. At this magnification a solidification structure becomes evident. The cracks appear to be present only in the outer covering which is probably an oxide film. Where the covering has cracked and broken away, a coarser solidification structure is seen. This structure is apparently due to metallic solidification in the bulk of the "blob". Features such as these most probably result from molten particles produced during abrasive cutting of samples and specimens from the fractured



(A) 200X



(B) 500X

Figure 35. SEM micrographs of "blob" found on an N-155 fracture surface.

welds. These molten particles fell or were propelled onto the fracture surfaces. These "blobs" are definitely not related to the fracture process and are true artifacts.

Often many completely spherical particles are found on the fracture surfaces. These spheres may range in size from 1 to 300  $\mu$ . The SEM micrographs in Figure 36 show one of the larger (300  $\mu$ ) spheres which is wedged in a crevice on a Waspaloy fracture surface. When viewed at higher magnification, the sphere appears as shown in Figure 36B. The surface appears to be oxidized. In an attempt to better understand these features, this specimen was nickel-plated and then carefully sectioned so that the internal structure of the sphere could be revealed. Figure 37A, a light micrograph at 100X, shows a cross sectional view of the sphere as it is located within the crevice. The surrounding gray material is the nickel-plating which was added to improve edge and sphere retention. The upper black region is a void space which is located entirely within the sphere. The black region is a void space where the nickel-plating did not completely fill the crevice. Figure 37B is a 500X magnification micrograph of the sphere. The arrow in Figure 37B indicates a thin oxide film which covers the sphere. The dark gray, circular areas within the sphere are probably oxide particles. ED spectrography indicated that some regions of the sphere contained high concentrations of chromium when compared to the base material. Again this feature is most

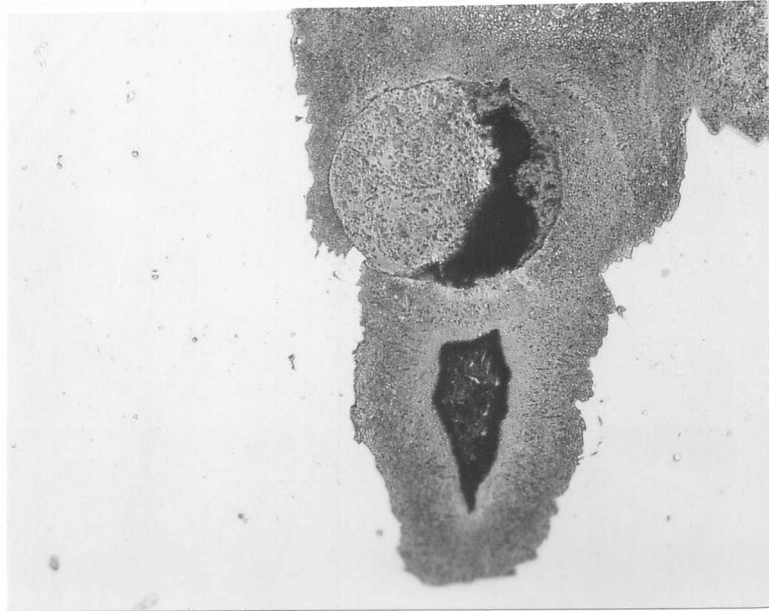


(A) 47X

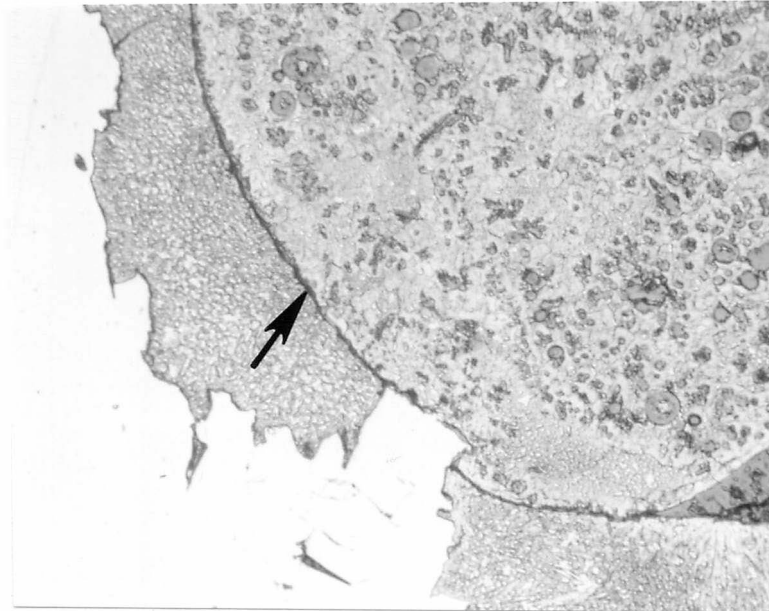


(B) 950S

Figure 36. SEM micrographs of large spherical particle.



(A) 100X



(B) 500X

Figure 37. Light micrographs of sphere shown in Figure 36.

probably the result of abrasive cutting which often produces molten particles. The fact that this feature is almost perfectly spherical and is coated by an oxidized film suggests that the sphere was formed and solidified during transit to the fracture surface. The crevice in which it was found served to retain it on the fracture surface.

Many smaller (1 to 10  $\mu$ ) spheres which were observed on the fracture surfaces differed in appearance from those previously discussed. These smaller spheres had essentially no oxide covering and the solidification structure was clearly observable over the entire surface. Two such small (1  $\mu$ ) spheres are shown in the SEM micrograph which appears in Figure 38. These spheres can be seen nestled within a depression. Figure 39A shows these same spheres at 5000X magnification. The solidification structure is plainly visible. An x-ray area map using iron-K $\alpha$  radiation for this same area is shown in Figure 39B. This x-ray area map qualitatively shows that the spheres are relatively high in iron when compared to the surrounding fracture surface.

A slightly larger and hollow sphere is shown in the SEM micrograph in Figure 40. ED spectrography of this sphere indicates high iron as compared to the surrounding fracture surface. Many hollow spheres were encountered in this study. The cavity within the sphere suggests that a gas or vapor phase played a role in its formation. The smaller



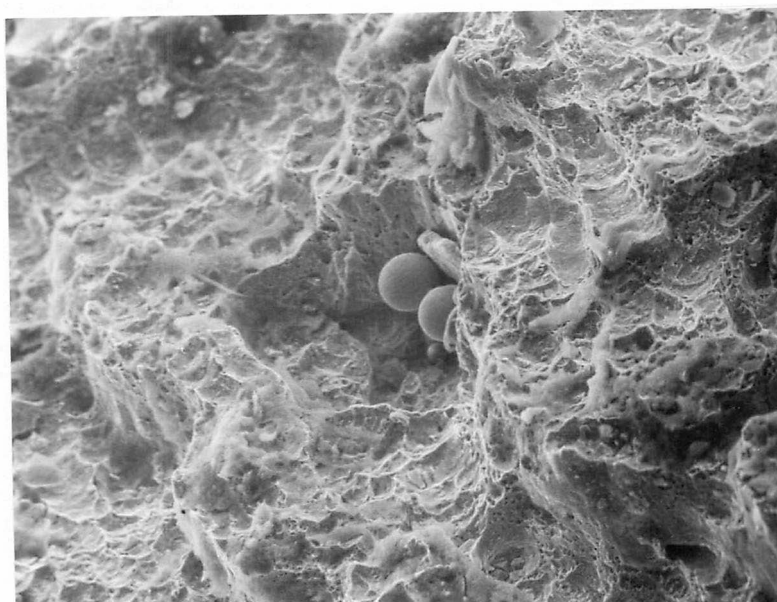
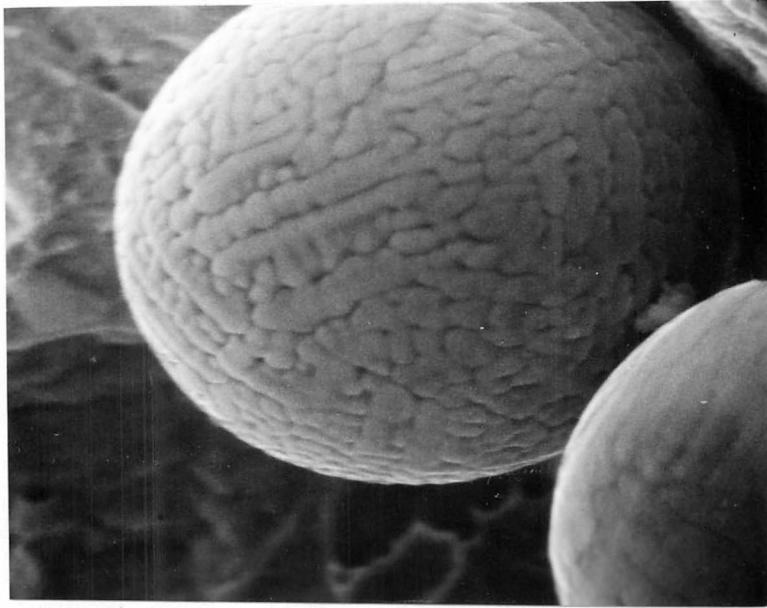
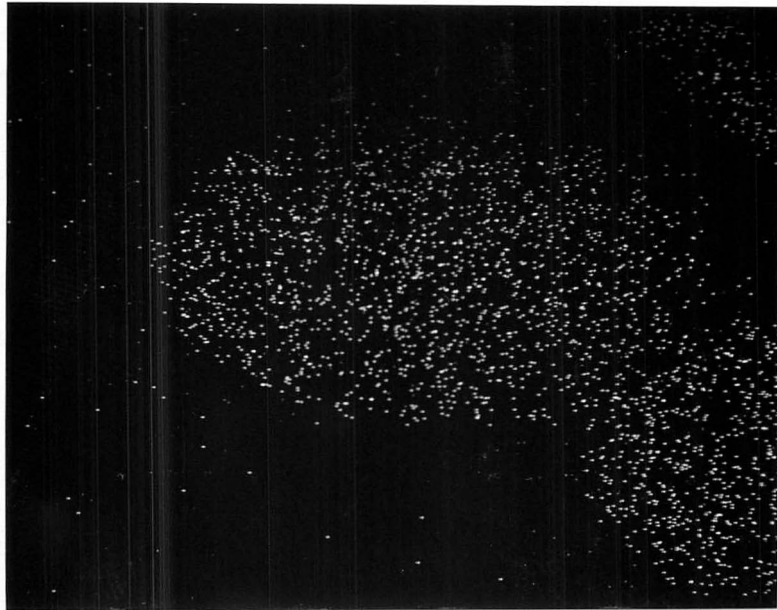


Figure 38. SEM micrograph of small spheres on fracture face of Inconel 625. 500X



(A) 5000X



(B) 5000X

Figure 39. High magnification SEM micrograph and iron-K  $\alpha$  radiation area map of spheres shown in Figure 38.

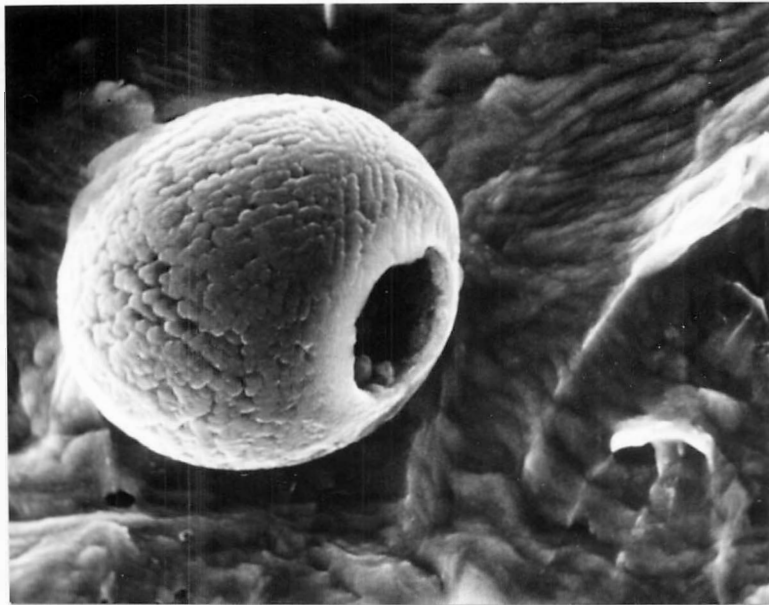


Figure 40. SEM micrograph of hollow sphere. 1000X

spheres (1 to 10  $\mu$ ) were numerous and not characteristic of any particular fracture mode, thus it is felt that spheres in this size range are inclusions or are the result of particle formation due to thermal effects in the base material. They are exposed during the fracture process.

## VITA

Ronald William Gunkel was born in Belleville, Illinois, on September 16, 1945. He attended elementary and high schools in Indianapolis, Indiana. In June 1967 he received a Bachelor of Science degree in Metallurgical Engineering from Purdue University. Upon graduation he was employed as a welding engineer by Oak Ridge National Laboratory. In March 1970 he began employment as a process engineer for the Stellite Division of Cabot Corporation.

In March 1972 he accepted a teaching assistantship at the University of Tennessee and began study toward a Master's degree. He received a Master of Science degree with a major in Metallurgical Engineering in June 1974. He is a member of the American Society for Metals and the American Welding Society.

He is married to the former Joyce Norton of New Market, Tennessee.